Experimental and Theoretical Studies of Bonding and Oxidative Addition of Germanes and Silanes, $EH_{4-n}Ph_n$ (E = Si, Ge; n = 0−3), to Mo(CO)(diphosphine)$_2$. The First Structurally Characterized Germane σ Complex

Jean L. Vincent,[†,⊥] Steven Luo,[†,⊥] Brian L. Scott,[†] Ray Butcher,[†,§] Clifford J. Unkefer,[†] Carol J. Burns,[†] Gregory J. Kubas,*[,†] Agusti Lledós,*[,‡] Feliu Maseras,[‡] and Jaume Tomàs[‡]

Chemistry Division, Los Alamos National Laboratory, MS J514, Los Alamos, New Mexico 87545, and Departament de Química, Universitat Autònoma de Barcelona, 08193 Bellaterra, Barcelona, Spain

Received August 7, 2003

Reaction of GeH_4 and GeH_3Ph with the agostic complex Mo(CO)(dppe)$_2$ (dppe = $Ph_2PC_2H_4PPh_2$) provides germane σ complexes Mo(CO)(η^2-$GeH_{4-n}Ph_n$)(dppe)$_2$ (n = 0, 1). The coordination in these complexes has been assigned as (η^2-Ge−H) on the basis of NMR and IR spectroscopy and by comparison to the analogous complexes of silanes. When the more electron-rich phosphine depe (depe = $Et_2PC_2H_4PEt_2$) is used, oxidative addition (OA) products $MoH(GeH_3)(CO)(depe)_2$ and $MoH(GeH_2Ph)(CO)(depe)_2$ are isolated (NMR and X-ray evidence). However, when the secondary organogermane GeH_2Ph_2 is used in the depe system, the η^2-complex Mo(CO)(η^2-GeH_2Ph_2)(depe)$_2$ is obtained. This complex was characterized by X-ray crystallography and NMR and IR spectroscopy. The Mo(CO)(η^2-GeH_3Ph)(dppe)$_2$ and Mo(CO)(η^2-GeH_2Ph_2)(depe)$_2$ complexes were found to be in tautomeric equilibrium with their OA products in solution. Structure and bonding comparisons are made to the analogous silane complexes, e.g., Mo(CO)(η^2-SiH_2Ph_2)(depe)$_2$, the X-ray structure for which is also reported. The Ge−H bonds undergo OA much more easily than Si−H, and to obtain further insight into the activation processes, ab initio DFT calculations have been performed on Mo(CO)($EH_{4-n}vin_n$)(dhpe)$_2$ model complexes (E = Si, Ge; n = 0−3; dhpe = $H_2PCH_2CH_2PH_2$; vin = CH=CH_2) and also the analogous H_2 complex. Because the ease of the whole OA process is a balance between the E−H bonding energy and Mo−E bonding energy, it can be concluded that the factor that makes OA of the Ge−H bond easier than that for Si−H is the relative weakness of the Ge−H bond, despite the fact that the Mo−Ge bond is also weaker. This competition between both factors is also seen for OA of H_2, for which although the Mo−H bonding energy is much higher than Mo−Si and Mo−Ge bonding energies, the H−H bond is also significantly stronger than the Si−H and Ge−H bonds. In general, the ease of OA of molecular hydrogen is between that of germanes and silanes. Calculations show that for alkanes the OA is much more difficult because the loss of the high C−H bond energy (comparable to or greater than that for H−H) is not as well compensated for by the energy of formation of the Mo−C bond due to the weakness of the Mo−C bond.

1. Introduction

The study of η^2-coordination of E−H σ bonds (X = H, C, Si, Ge, etc.) to unsaturated transition metal complexes is of fundamental importance both from a structure/bonding point of view and as a model for the activation of E−H bonds toward either homolytic or heterolytic cleavage.[1] These σ complexes can be viewed as "snapshots" at various points along the reaction coordinate for oxidative addition (OA) of an E−H bond to a metal center, i.e., formation of $L_nMH(E)$.

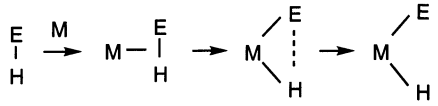

Consequently, studies that shed light on the structure and reactivity of these complexes provide valuable insight into the factors that influence catalytic transformations of H_2, organosilanes, organogermanes, and potentially most importantly, alkanes. Indeed direct

* To whom correspondence should be addressed. E-mail: kubas@lanl.gov; agusti@klingon.uab.es.
† Los Alamos National Laboratory.
⊥ Present addresses: J.L.V.: Electronics Technology−R1103, Air Products and Chemicals, 7201 Hamilton Blvd., Allentown, PA 18195; S.L.: Central Research Department, Bridgestone/Firestone Inc., 1200 Firestone Parkway, Akron, OH 44317.
§ Permanent address: Department of Chemistry, Howard University, Washington, DC 20059.
‡ Universitat Autónoma de Barcelona.

(1) (a) *Metal Dihydrogen and σ-Bond Complexes*; Kubas, G. J.; Kluwer Academic/Plenum Publishers: New York, 2001. (b) Kubas, G. J. *J. Organomet. Chem.* **2001**, *653*, 37. (c) Crabtree, R. H. *Angew. Chem., Int. Ed. Engl.* **1993**, *32*, 789.

10.1021/om030569j CCC: $25.00
Publication on Web 11/06/2003

transfer of the proton from an η^2-E−H ligand to a substrate may be a key step in catalysis.[1a] There are many examples of η^2-E−H σ complexes for E = H, a moderate number for E = Si[1,2] and Sn,[1,3] but few for transition metal complexes with η^2-coordinated Ge−H bonds. For the lightest group 4 congener, E = C, stable alkane complexes are yet unknown, although agostically coordinated C−H bonds are common, as exemplified below. Note however that *agostic* refers to *intra*molecular interactions and should not be used to describe *inter*molecular σ-ligand coordination, which should be referred to as σ complexes.

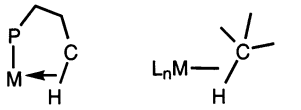

As was the case for preparation of analogous η^2-Si−H complexes,[2a] the photolytically generated 16e $CpMn(CO)_2$ fragment was a useful precursor for synthesizing germane complexes (eq 1), where the bound germanes were $GeHPh_3$ and GeH(Me)(Ph)(naphthyl).[4]

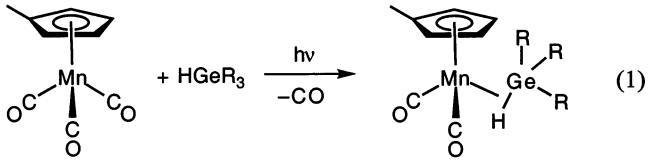

(1)

Although X-ray and NMR evidence were not obtained, the properties and reactivities are similar to silane analogues. As for M(η^2-Si−H), photoelectron spectroscopy studies (PES) confirm interaction of the Ge−H σ and σ* orbitals with M.[5] The electronic structure of the interaction is consistent with an early stage of Ge−H bond addition to M, and donation of Ge−H electrons to M predominates over back-donation. In comparison to the silane analogue, $MeCpMn(CO)_2(SiHPh_3)$, the Cp and M ionization energies are at nearly the same position, indicative of similar charges on the Mn centers. The Si−H and Ge−H σ interactions with Mn are nearly the same in magnitude. However, the extent of back-donation appears to be slightly higher in M(η^2-Ge−H), consistent with the situation in Mo complexes discussed below and the expectation that the Ge−H σ* level is lower in energy than that of the corresponding Si−H σ* orbital.

The complexes $RuH_2(H_2)(EHPh_3)(PCy_3)_2$ (E = Si, Ge) have been reported, although the germane complex was not structurally characterized.[6] A dimer containing Cp_2-Ti centers isolated as an intermediate in the dehydrocoupling reaction of GeH_2Ph_2 with Cp_2TiMe_2 is proposed to have either one or two bridging $GeHPh_2$ units from NMR data.[7] Related dinuclear germyl-bridged Fe complexes provide the first structural evidence for M···H−Ge interaction, although they are agostic in nature.[8]

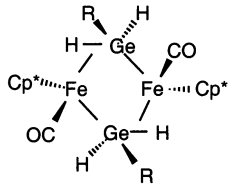

The Ge−H distance is 2.03(8) Å, which is significantly longer than the normal length of 1.529 Å,[9] and the Fe−H distance is 1.64(16) Å. The IR stretch for the coordinated Ge−H bond occurs at 1849−1898 cm^{-1}.

We now report coordination of germanes to Mo(CO)-$(PP)_2$ (PP = diphosphine), including the first examples of a GeH_4 complex and a crystal structure of a η^2-Ge−H transition metal σ complex. η^2-Ge−H coordination as well as activation of Ge−H bonds toward OA has been established to be similar to that for silane σ complexes such as $Mo(CO)(SiH_{4-n}R_n)(PP)_2$ (n = 0−3). The structure, bonding, and spectroscopic properties of the latter, including the first transition metal SiH_4 complex, have been previously studied by us[10,11] and compared to analogous σ complexes such as the H_2 and agostic C−H complexes, $Mo(CO)(H_2)(PP)_2$[12] and $Mo(CO)(PP)_2$.[13,14]

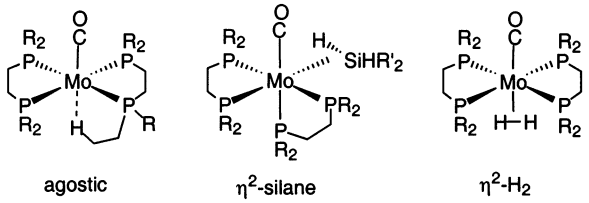

The Mo complexes offer the only direct structural comparison of the coordination of H−H, C−H, Si−H, and Ge−H σ bonds. In addition, we report here DFT-based theoretical calculations on these systems that compare the bonding and activation of Ge−H, Si−H, H−H, and C−H bonds with experimental findings. The degree of activation of the coordinated germane or silane toward OA is finely controlled by substituents on both the phosphine ligands and at Ge or Si.

(2) (a) Schubert, U. *Adv. Organomet. Chem.* **1990**, *30*, 151. (b) Corey, J. Y.; Braddock-Wilking, J. *Chem. Rev.* **1999**, *99*, 175. (c) Lin, Z. *Chem. Soc. Rev.* **2002**, *31*, 239. (d) Nikonov, G. I. *J. Organomet. Chem.* **2001**, *635*, 24.

(3) (a) Schubert, U.; Kunz, E. K.; Harkers, B.; Willnecker, J.; Meyer, J. *J. Am. Chem. Soc.* **1989**, *111*, 2572. (b) Beagley, B.; McAloon, K.; Freeman, J. M. *Acta Crystallogr., Part B* **1974**, *30*, 444. (c) Piana, H.; Kirchgaessner, U.; Schubert, U. *Chem. Ber.* **1991**, *124*, 743. (d) Khaleel, A.; Klabunde, K. J. *Inorg. Chem.* **1996**, *35*, 3223. (e) Carleton, L. *Inorg. Chem.* **2000**, *39*, 4510. (f) Carleton, L.; Weber, R.; Levendis, D. C. *Inorg. Chem.* **1998**, *37*, 1264. (g) Carleton, L. *Appl. Organomet. Chem.* **2001**, *15*, 157. (h) Carleton, L. *South African J. Sci.* **2001**, *97*, 76.

(4) Carre, F.; Colomer, E.; Corriu, R. J. P.; Vioux, A. *Organometallics* **1984**, *3*, 1272.

(5) Lichtenberger, D. L.; Rai-Chaudhuri, A. *J. Chem. Soc., Dalton Trans.* **1990**, 2161.

(6) Sabo-Etienne, S.; Hernandez, M.; Chung, G.; Chaudret, B.; Castel, A. *New J. Chem.* **1994**, *18*, 175.

(7) Aitken, C.; Harrod, J. F.; Malek, A.; Samuel, E. *J. Organomet. Chem.* **1988**, *349*, 285.

(8) (a) El-Maradny, A.; Tobita, H.; Ogino, H. *Organometallics* **1996**, *15*, 4954. (b) Tobita, H.; Ogino, H., private communication.

(9) Emsley, J. *The Elements*; Clarendon Press: Oxford, 1989.

(10) Luo, X.-L.; Kubas, G. J.; Bryan, J. C.; Burns, C. J.; Unkefer, C. J. *J. Am. Chem. Soc.* **1994**, *116*, 10312.

(11) Luo, X.-L.; Kubas, G. J.; Burns, C. J.; Bryan, J. C.; Unkefer, C. J. *J. Am. Chem. Soc.* **1995**, *117*, 1159.

(12) (a) Kubas, G. J.; Ryan, R. R.; Wroblewski, D. *J. Am. Chem. Soc.* **1986**, *108*, 1339. (b) Kubas, G. J.; Ryan, R. R.; Unkefer, C. J. *J. Am. Chem. Soc.* **1987**, *109*, 8113. (c) Kubas, G. J.; Burns, C. J.; Eckert, J.; Johnson, S.; Larson, A. C.; Vergamini, P. J.; Unkefer, C. J.; Khalsa, G. R. K.; Jackson, S. A.; Eisenstein, O. *J. Am. Chem. Soc.* **1993**, *115*, 569. (d) Luo, X.-L.; Kubas, G. J.; Burns, C. J.; Eckert, J. *Inorg. Chem.* **1994**, *33*, 5219.

(13) Sato, M.; Tatsumi, T.; Kodama, T.; Hidai, M.; Uchida, T.; Uchida, Y. *J. Am. Chem. Soc.* **1978**, *100*, 4447.

(14) Luo, X.-L.; Kubas, G. J.; Burns, C. J.; Butcher, R. J.; Bryan, J. C. *Inorg. Chem.* **1995**, *34*, 6538.

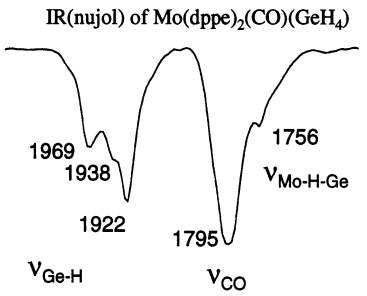

Figure 1. Nujol mull IR spectrum (cm^{-1}) of Mo(CO)-(GeH_4)(dppe)$_2$.

Table 1. IR Stretches for Germane and Germyl Hydride Complexes Compared to Silane Analogues

complex	ν(E−H)	ν(Mo−H−E)	ν(CO)
Mo(CO)(η^2-GeH_4)(dppe)$_2$ (**1**)	1969, 1938, 1922	1756	1795
Mo(CO)(η^2-SiH_4)(dppe)$_2$	2081, 2028, 2000	1743	1783
Mo(CO)(η^2-SiH_4)(depe)$_2$	2047, 1995, 1972	1732	1775
MoH(GeH_3)(CO)(depe)$_2$ (**2**)	1928, 1887, 1857	1728[a]	1756
MoH(GeH_2Ph)(CO)(depe)$_2$ (**4**)	1872, 1856	1720[a]	1759
Mo(CO)(η^2-GeH_2Ph_2)(depe)$_2$ (**3**)	1838	1757	1780
Mo(CO)(η^2-SiH_2Ph_2)(depe)$_2$	2010	1752	1792

[a] ν(Mo−H).

2. Synthesis and Characterization of Germane and Germyl Hydride Complexes

2.1. Mo(CO)(η^2-GeH_4)(dppe)$_2$, 1, and MoH(GeH_3)-(CO)(depe)$_2$, 2. Synthesis of the Mo-η^2-GeH_4 complex, **1**, proceeds according to eq 2 to give pale yellow **1** in 49% yield.

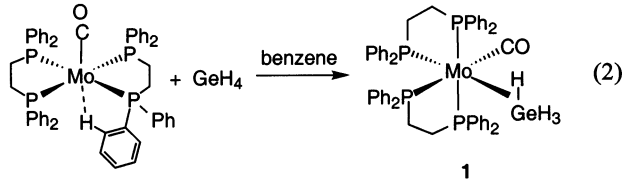

(2)

1

Although crystals for X-ray diffraction could not be obtained because of the low solubility of **1**, the IR spectrum (Figure 1) is very similar to that for a η^2-SiH_4 analogue, for which X-ray crystallography[11] shows octahedral coordination as depicted for **1** in eq 2. Complex **1** is insoluble in or decomposed in every common solvent except THF-d_8, in which it was slightly soluble, thereby allowing a ^{1}H NMR (but not ^{31}P) spectrum to be obtained. A broad signal appeared at −5.90 ppm presumably due to Mo−H−Ge (cf. −6.87 ppm for the η^2-SiH_4 analogue in C_6D_6[11]). A very broad multiplet for the unbound GeH_3 protons appeared at 4.4−5.5 ppm (cf. 4.46 ppm for the η^2-SiH_4 analogue). In these complexes the η^2-EH_4 is regarded as a single ligand with the midpoint of one E−H σ bond occupying a coordination site cis to CO (E = Si, Ge). The involvement of only one GeH_4 hydrogen rather than potentially two or three in the bonding to Mo is suggested by the IR of solid **1**, which shows three bands for the terminal Ge−H groups and one for the Mo−H−Ge stretch for the three-center σ interaction at 1756 cm^{-1} (Table 1 compares the data with that for the SiH_4 complex). The single fundamental Ge−H stretch in free GeH_4[15] at 2111 cm^{-1} is thus split into three terminal Ge−H bands and one Mo−H−Ge "bridging" mode at lower frequencies on coordination. It should also be noted that ligand rearrangement occurs in eq 2, and the CO originally trans to the "open site" (weakly occupied by the agostic C−H interaction) is now presumably cis to the η^2-GeH_4 ligand in **1**, as supported by calculations discussed below. A similar rearrangement occurs for SiH_4 coordination, as shown in the X-ray structure of *cis*-Mo(CO)(η^2-SiH_4)(^{i}Bu$_2$PC_2H_4P^i-Bu$_2$)$_2$.[11] The positions of νCO and ν(Mo−H−E) are similar for **1** and *cis*-Mo(CO)(η^2-SiH_4)(dppe)$_2$ (Table 1).

For the more electron-rich depe analogue, OA of GeH_4 occurs according to eq 3, where the labile μ-N_2 ligand of the synthetically useful dinuclear precursor complex[14] is presumably displaced by germane, and a Ge−H bond cleaves on the electron-rich Mo to give the germyl hydride.

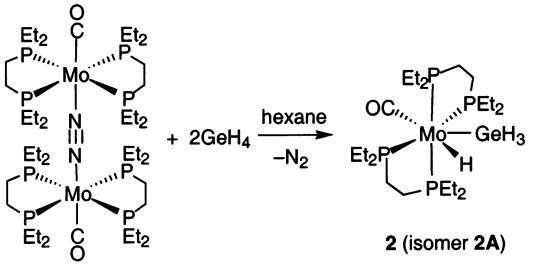

(3)

2 (isomer **2A**)

Although X-ray data could not be obtained for MoH-(GeH_3)(CO)(depe)$_2$, **2**, the formulation as a germyl hydride rather than a σ complex is based primarily on IR data (Table 1). On comparison to those for **1**, the IR frequencies ν(Ge−H), ν(Mo−H−Ge), and ν(CO) are all 28−61 cm^{-1} lower for **2**, consistent with OA of GeH_4. The corresponding band difference for SiH_4 binding to the dppe versus depe fragments is only 8−34 cm^{-1}, which presumably represents the electronic influence of changing the phosphine basicity. Significantly, the bands for **2** are quite similar to those for MoH($PhGeH_2$)-(CO)(depe)$_2$ (**4**), which is known to be a germyl hydride from X-ray data discussed below. The NMR of **2** in solution indicates the presence of two isomers. Both at room temperature and at low temperature (−80 °C), ^{31}P-{^{1}H} NMR shows four signals in the 34−85 ppm range assigned as isomer **2A** (three singlets in 1:2:1 ratio) and isomer **2B** (singlet at 66.3 ppm). The ratio of **2A** to **2B** at −80 °C from signal integration is 4.8:1 but becomes closer to 2:1 on warming to RT (the resonances for **2A** broaden, and all signals shift slightly). This behavior differs from that for Mo(CO)(SiH_4)(depe)$_2$, which shows four singlets at RT for the η^2-SiH_4 tautomer plus an additional four singlets on cooling that result from freezing out the fluxional seven-coordinate silyl hydride tautomer in equilibrium with the σ complex (eq 4).[11]

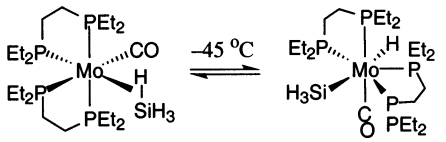

(4)

η² **oa**

4 ^{31}P signals, δ 39-67 4 ^{31}P signals, δ 35-83

The 1:2:1 ^{31}P NMR pattern for **2A** could be assignable to a MoH(GeH_3)(CO)(depe)$_2$ species with a pentagonal

(15) Lin, H.; Wang, D.; Chen, X.-Y.; Wang, X.-G.; Zhou, Z. P.; Zhu, Q.-S. *J. Mol. Spectrosc.* **1998**, *192*, 249.

bipyramidal structure as shown in eq 3, where the H and GeH_3 are proximal rather than distal as for the silyl hydride in eq 4. If the CO lies in the pentagonal plane, the two axial P atoms may become chemically equivalent if the complex has some degree of stereochemical nonrigidity, as is common[16] for such seven-coordinate species. The 51 ppm range of chemical shifts for the ^{31}P peaks of **2A** (34−85 ppm) is consistent with a seven-coordinate OA structure as for $MoH(SiH_3)(CO)(depe)_2$. Generally, OA products of the type $MoH(ER_3)(CO)(diphosphine)_2$ have a ^{31}P range of about 50 ppm, while the corresponding η^2-HER_3 complexes have a range of about 30 ppm, as exemplified by the silane system[11] in eq 4 and the organogermane complexes below (eq 6). Isomer **2B** could be a highly fluxional seven-coordinate species with a single, averaged $^{31}P\{^1H\}$ resonance both at RT and −80 °C. Capped trigonal prismatic geometries are also possible for these isomers.

The proton NMR of complex **2** at −80 °C shows a quintet at −7.59 ppm ($J_{HP} = 41.3$ Hz) assignable to the hydride ligand of **2B** (four equivalent phosphorus) and a multiplet centered at −7.85 ppm due to the hydride in **2A**. These spectral features are quite similar to those observed at RT for the crystallographically characterized hydrido-phenyl germyl complex, $MoH(PhGeH_2)(CO)(depe)_2$ (**4**), discussed below. The ^1H spectrum of **2** at RT shows a multiplet (triplet superimposed over a broad, flat-top resonance) centered at −7.8 ppm presumably due to isomer **2A**, consistent with the presence of two equivalent axial phosphorus atoms as in the structural representation in eq 3. A signal for **2B** could not be identified, which would be consistent with a highly fluxional seven-coordinate species. Singlet resonances for the GeH_3 ligand are observed at 3.27 and 2.56 ppm respectively for **2A** and **2B** at −80 °C. These are both at higher field than for the unbound GeH_3 protons in the η^2-GeH_4 complex, **1**, indicating that both **2A** and **2B** are isomers of a germyl hydride rather than η^2-GeH_4 complexes.

2.2. Organogermane Complexes. Addition of either diphenylgermane or diphenylsilane to $Mo(CO)(dppe)_2$ in toluene gives no reaction, possibly because of steric crowding. However reaction does occur in both cases for the more electron-rich depe system where Mo→E−H back-bonding is stronger and there is less steric crowding. Equation 5 shows the results for the germane system and the dramatic effect of a relatively minor change of substituent on the germane which induces the complex to undergo OA (**4**).

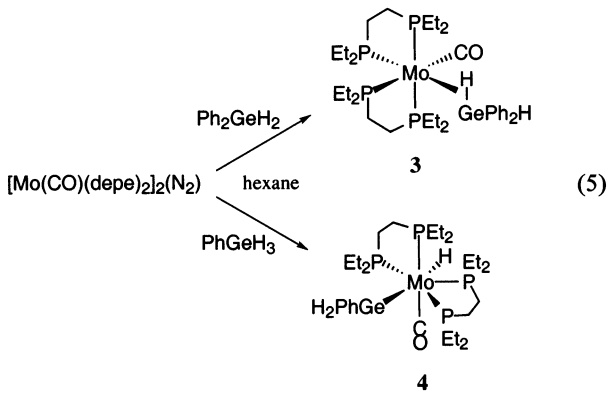

3 (5)

4

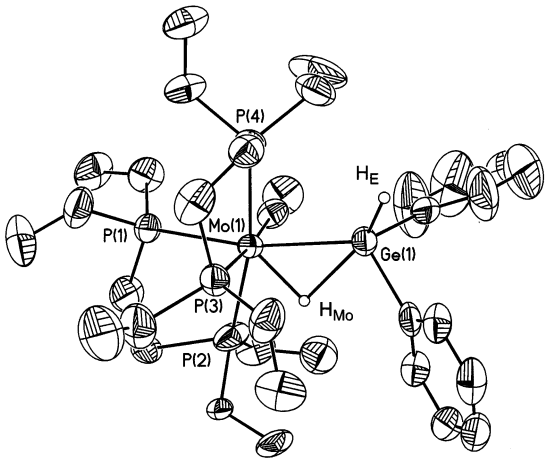

Figure 2. Thermal ellipsoid plot (35% probability ellipsoids) of $Mo(CO)(GeH_2Ph_2)(depe)_2$, **3**. Hydrogen atom positions on germanium have been located on a difference map and refined.

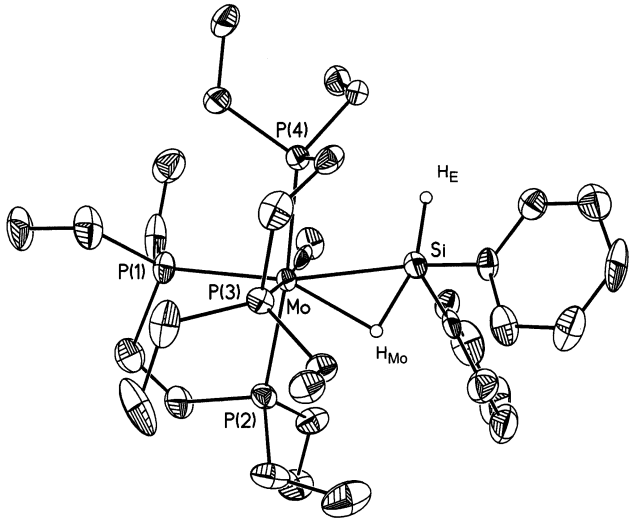

Figure 3. Thermal ellipsoid plot (50% probability ellipsoids) of $Mo(CO)(SiH_2Ph_2)(depe)_2$. Hydrogen atom positions on Si have been located on a difference map and refined.

The solid product of the reaction with GeH_2Ph_2 is the yellow σ complex **3**, which has the octahedral structure shown in eq 5 according to X-ray data (Figure 2). As for the organosilane analogue which has a similar X-ray structure (Figure 3), one terminal X−H stretch and one Mo−H−X stretch are seen in the IR (Table 1) as expected. νCO is higher for the germane σ complexes than the silane congeners, possibly because of greater back-donation to the Ge−H bond and/or lower σ donation from Ge−H, as will be discussed below. In contrast to the reaction with GeH_2Ph_2, the product of the reaction with the *monosubstituted* germane, $GeHPh_3$, is the *OA product*, **4**, which has the pentagonal bipyramidal X-ray structure in eq 5 (Figure 4, where CO and P(3) lie in the axial positions). The rationale for the difference in reaction products (germyl hydride versus σ complex) is electronic, as discussed in section 4. The NMR of **4** is consistent with the solid-state structure (four ^{31}P resonances both at −80 °C and RT) but also shows the presence of a minor isomer **4B** at RT, which diminishes

(16) Luo, X.-L.; Schulte, G. K.; Demou, P.; Crabtree, R. H. *Inorg. Chem.* **1990**, *29*, 4268, and references therein.

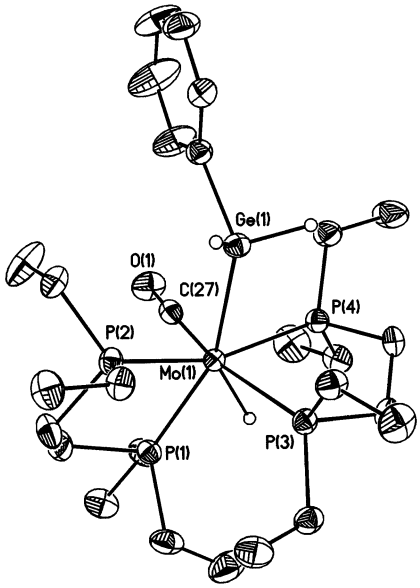

Figure 4. Thermal ellipsoid plot (35% probability ellipsoids) of $MoH(GeH_2Ph)(CO)(depe)_2$, **4**. Hydrogen atom positions on Mo and Ge have been located on a difference map and refined. CO and P(3) are the axial ligands in the pentagonal bipyramid. Selected bond distances (Å) and angles (deg): Mo−H, 1.716(39); Mo−C(27), 1.924(3); Mo−P(1), 2.4235(8); Mo−P(4), 2.4585(9); Mo−P(2), 2.4934(9); Mo−P(3), 2.5627(8); Mo−Ge, 2.6693(5); Ge−C(21), 1.998(3); O(1)−C(27), 1.189(3); C(27)−Mo−P(1); 82.60(9); C(27)−Mo−P(4), 85.34(9); P(1)−Mo−P(4); 123.08(3); C(27)−Mo−P(2), 95.59(9); P(1)−Mo−P(2), 78.32(3); P(4)−Mo−P(2), 158.40(3); C(27)−Mo−P(3), 165.49(9); P(1)−Mo−P(3), 103.61(3); P(4)−Mo−P(3), 80.28(3); P(2)−Mo−P(3), 98.50(3); C(27)−Mo−Ge, 93.98(9); P(1)−Mo−Ge, 155.15(2); P(4)−Mo−Ge, 80.87(2); P(2)−Mo−Ge, 77.53(2); P(3)−Mo−Ge, 85.72(2); C(21)−Ge−Mo, 123.86(9); O(1)−C(27)−Mo, 175.3(3); H−Mo−P(4), 67(1); H−Mo−P(1), 59(1); H−Mo−P(3), 76(1).

at low temperature and shows only one ^{31}P signal. This solution tautomeric behavior and the NMR spectral features are very similar to those seen for $MoH(GeH_3)(CO)(depe)_2$ (**2**) above. The IR of **4** is closer to that of **2** than that for the germane σ complexes (e.g., lower νCO, Table 1).

In solution, **3** shows tautomeric equilibrium between the σ complex **3-η²** and the germyl hydride **3-oa** formed by reversible OA of the Ge−H bond (eq 6). ^1H and ^{31}P-

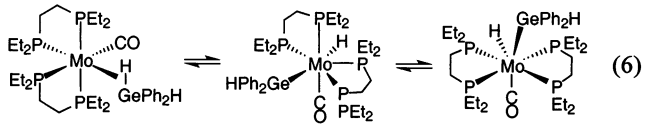

{^1H} NMR spectroscopy (Figures 5 and 6) show distinct signals for these tautomers at −80 °C (denoted by a for **3-oa** and b for **3-η²**). There is also a third set of peaks (c) at −80 °C for an isomer, **3-x**, that may have a trigonal-like MoH(Ge)(CO) geometry with the diphosphines in an orthogonal plane. This is consistent with only two ^{31}P signals and a quintet-like pattern near δ −7 in the ^1H NMR at intermediate temperatures (Figure 5), indicative of ^{31}P coupling to a hydride ligand by four phosphorus atoms that could become equivalent

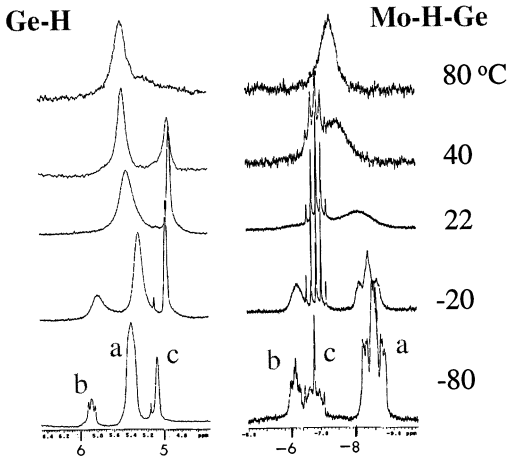

Figure 5. ^1H NMR spectra (C_7D_8, −80 °C) of **3** showing distinct signals for tautomers (denoted by a for **3-oa** and b for **3-η²**). There is also a third set of peaks (denoted by c) for an isomer of unknown structure, **3-x.**

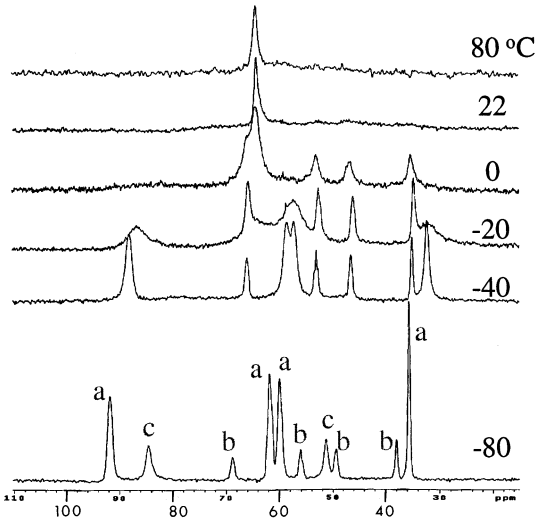

Figure 6. ^{31}P NMR spectra (C_7D_8, −80 °C) of **3** showing distinct signals for tautomers (denoted by a for **3-oa** and b for **3-η²**). There is also a third set of peaks (denoted by c) for an isomer of unknown structure, **3-x.**

at 40 to −20 °C because of fluxionality. Note that consistent with this, the ^{31}P spectra (Figure 6) show that the two peaks (c) seen at −80 °C assigned to **3-x** coalesce in this temperature range to one peak near δ 66, which is still visible at 0 °C as a shoulder on the δ 66 peak. **3-x** could have a highly elongated Ge−H bond much like in elongated H_2 complexes.[1] The ^{31}P peaks for **3-η²** and **3-oa** are assigned on comparison to the spectra (Figure 7) for the analogous $Mo(CO)(dppe)_2(GeH_3Ph)$ system, **5-η²** ↔ **5-oa**, which does not show a third isomer (eq 7).

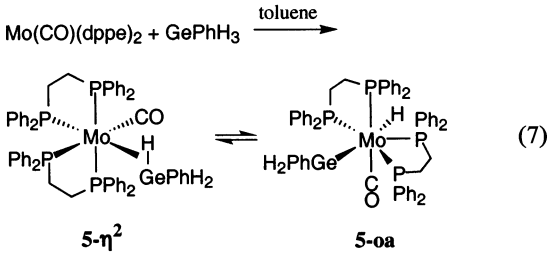

Although a solid product was not isolated for the reaction of phenylgermane with the less electron-rich

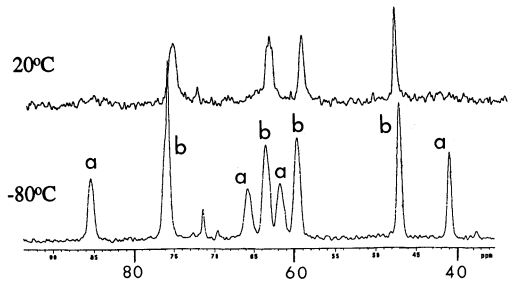

Figure 7. ^{31}P NMR spectra (C_7D_8, −80 °C) of Mo(CO)(η^2-GeH_3Ph)$(dppe)_2$, **5**, showing distinct signals for tautomers (denoted by a for **5-oa** and b for **5-η^2**).

and sterically bulkier dppe complex, NMR spectra show two sets of signals consistent with a ratio of **5-η^2** to **5-oa** of 1.5. ^{31}P{^{1}H} spectra at 20 °C do not display signals for **5-oa** because it is highly fluxional and the signals are presumably coalesced. Decoalescence to four signals (denoted as a in Figure 7) does occur on cooling to −80 °C, consistent with the expected inequivalent phosphorus atoms. Four separate singlets (b) are present at both room and low temperatures for the tautomer, **5-η^2**, which is a stereochemically rigid octahedral σ complex. This behavior is much like that observed for a similar tautomeric equilibrium for the silane complex *cis*-Mo(CO)(η^2-SiH_4)$(depe)_2$ (eq 4).[11] The ^{1}H resonance at −80 °C for the hydrogen atom in the coordinated η^2-Ge−H bond in **5-η^2** is a broad singlet at δ −5.06, while the singlet hydride resonance for **5-oa** is nearby at δ −5.25. By comparison, the corresponding hydride-region resonances in the *diphenyl*germane system (the three isomers of **3**) are all complex multiplets that are more widely spaced (Figure 5).

Attempts to deprotonate the germane ligand in **3** using reagents such as $[Ph_3C][BAr_F]$ led to disproportionation reactions and products not containing germyl ligands. Reactions with cyclooctene were not clean either, and disproportionation products also formed along with some cyclooctane. Displacement of the η^2-GeH_2Ph_2 ligand in **3** by GeH_3Ph occurred in benzene to give the germyl hydride OA product, **4**.

3. Thermodynamic Studies of Silane Binding and Activation

Few measurements of the binding energies and thermodynamics of activation of σ ligands other than H_2 have been made on stable complexes.[1] ^{31}P NMR measurements were thus carried out on reaction of SiH_2Ph_2 with an agostic Mo complex, Mo(CO)(^{i}Bu$_2$PC$_2$H$_4$P^{i}Bu$_2$)$_2$ (eq 8), in order to determine the energetics.

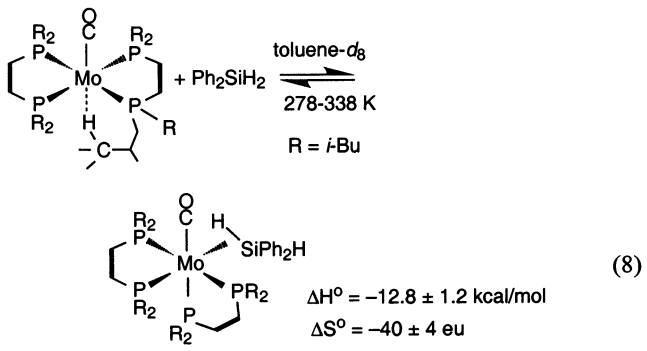

(8)

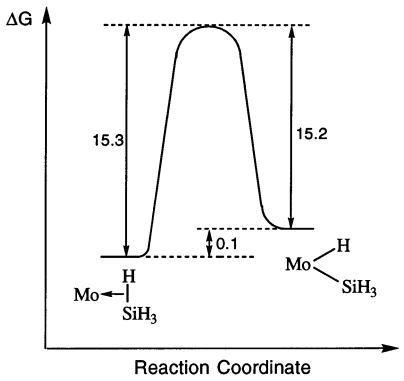

Figure 8. Free energy profile for equilibrium Mo(CO)(η^2-SiH_4)$(depe)_2$ ↔ MoH(SiH_3)(CO)$(depe)_2$ at 333 K, with ΔG values in kcal/mol.

The −12.8 kcal/mol binding enthalpy is very similar to that for H_2 binding to W$(CO)_3(PCy_3)_2$, −10 kcal/mol. The energy of the agostic interaction[14] in Mo(CO)(^{i}Bu$_2$PC$_2$H$_4$P^{i}Bu$_2$)$_2$ must be added on to give the true binding enthalpy of the σ ligands here, but is unknown (as for that in W$(CO)_3(PCy_3)_2$, which is estimated to be 5−10 kcal/mol[17]).

The equilibrium, Mo$(CO)(SiH_4)(depe)_2$ ↔ MoH(SiH_3)-$(CO)(depe)_2$, in eq 4 is readily amenable to thermodynamic analysis by variable-temperature ^{1}H NMR studies, and K_{eq} = 1 at 288 K. The thermodynamic parameters, $\Delta H° = -0.61 \pm 0.2$ kcal/mol and $\Delta S° = -2.1 \pm 0.7$ eu, were determined by van't Hoff plots of ln K_{eq} versus $1/T$. Although the OA product is slightly favored enthalpically here, related M(η^2-H_2) ↔ MH_2 equilibria can favor either the OA product or the σ complex by up to 1.7 kcal/mol depending on the metal−ligand set. There is virtually no free energy difference between the σ complex and the silyl hydride at RT, and the overall reaction profile (Figure 8) is very similar to that for the equilibrium W$(CO)_3(PR_3)_2(H_2)$ ↔ $WH_2(CO)_3$-$(PR_3)_2$, where $\Delta G^‡$ is 16.0 ± 2 kcal/mol at 298 K for R = ^{i}Pr.[18] Here the ground-state enthalpy favors the H_2 complex by 1.2 ± 0.6 kcal/mol, with a similarly negligible $\Delta S°$ of 1 eu. The K_{eq} at 298 K for H−H rupture on W$(CO)_3(PR_3)_2$ is 0.25 for R = ^{i}Pr, 0.29 for R = cyclopentyl, and 0.66 for R = Cy,[18] compared to 0.97 for Si−H bond cleavage on Mo.

Other experimental data such as J_{SiH} and the theoretical work discussed below imply that silane and germane complexes generally lie further along the reaction coordinate toward cleavage than H_2 complexes and that there may be other subtle differences in the nature of the σ bonding and activation. However the above thermodynamics of binding/cleavage of Si−H bonds on group 6 complexes compare very favorably to that for H_2 activation on group 6 and other systems, suggesting that the σ interactions and the homolytic σ-bond cleavage processes are fundamentally similar for Si−H and H−H.

(17) Gonzalez, A. A.; Zhang, K.; Nolan, S. P.; de la Vega, R. L.; Mukerjee, S. L.; Hoff, C. D.; Kubas, G. J. *Organometallics* **1988**, *7*, 2429.
(18) Khalsa, G. R. K.; Kubas, G. J.; Unkefer, C. J.; Van Der Sluys, L. S.; Kubat-Martin, K. A. *J. Am. Chem. Soc.* **1990**, *112*, 3855.

Table 2. Interatomic Distances and Angles for Mo(CO)(depe)$_2$(η^2-EH$_2$Ph$_2$) [E = Si (Figure 3), Ge (Figure 2)] (H_{Mo} = H bonded to Mo; H_E = H bonded to E)

	E = Si	E = Ge
	Distances, Å	
Mo−CO	1.952(8)	1.932(6)
Mo−P(1)	2.545(2)	2.5215(14)
Mo−P(2)	2.482(2)	2.4190(16)
Mo−P(3)	2.599(2)	2.5382(15)
Mo−P(4)	2.496(2)	2.5100(14)
Mo-E	2.563(3)	2.6368(7)
Mo−H_{Mo}	2.04(2)	1.72(6)
E−H_E	1.54(6)	1.49(7)
E−H_{Mo}	1.66(6)	2.08(6)
E−C_{Ph}	1.921(9),1.939(8)	2.019(3), 2.016(4)
C−O	1.188(8)	1.178(6)
	Angles, deg	
P(1)−Mo−E	154.37(9)	168.35(4)
P(2)−Mo−P(4)	173.73(8)	169.27(6)
P(3)−Mo−CO	174.7(2)	172.92(18)
E−Mo−H_{Mo}	40.3(12)	52(2)
Mo−E−H_{Mo}	52.6(11)	40.5(17)
H_{Mo}−E−H_E	161(2)	152(3)
Ph−E-Ph	103.0(4)	99.15(17)

Table 3. Comparison of Products of Reaction of Silane and Germane Analogues with Mo(CO)($R_2PC_2H_4PR_2$)$_2$ Precursor Fragments[a]

R	silane	J_{SiH} (Hz)[b]	structure[c]	structure of germane analogue[c]
Et	SiH_4	35	η^2/equil	OA
Et	SiH_3Ph	39	η^2	OA
Et	SiH_3(*n*-hexyl)	42	η^2	
Et	SiH_2Ph_2	50	η^2	η^2/equil
Ph	SiH_4	50	η^2	η^2[d]
Ph	SiH_3Ph	57	η^2 (unisolated)	equil[e]
Ph	SiH_3(*n*-hexyl)	61	η^2 (unisolated)	
Ph	SiH_2Ph_2		N.R.	N.R.

[a] All silane complexes are σ complexes in both solid and solution, and J_{SiH} values are listed. Product stability and tendency toward OA decrease down the table. [b] J_{SiH} for η^2-bound Si−H bonds. [c] η^2 = σ complex; OA = oxidative addition to germyl hydride; η^2/equil = η^2 in solid, but tautomeric equilibrium between OA and η^2 isomers in solution. [d] In solid; too insoluble for solution study. [e] Solid not isolated, equilibrium in solution.

4. X-ray Structures, Bonding, and Activation of Germane versus Silane Complexes: Effects of Substituents at the Phosphines and at Ge and Si

The degree of activation of the coordinated germane or silane toward OA is finely tuned by substituents both on the diphosphine ligands and at Ge or Si.[1,2] The substituents on phosphorus, e.g., alkyl versus aryl, can increase the electron-richness of the metal center and thus the M to σ-ligand back-donation, ultimately causing complete rupture of the σ bond.[1] On the other hand, decreasing the number of electron-donating substituents on E = Si or Ge (e.g., replacing R by H) increases the E−H activation and favors OA over formation of the σ complex, presumably because the EH σ* orbital energy is lowered, which favors more back-donation. These principles are well illustrated by a comparison of the products of silane and germane reactions with Mo(CO)-($R_2PC_2H_4PR_2$)$_2$ fragments (Table 3). For example, for silane complexes, electron-donating substituents such as alkyl or aryl groups decrease the Si−H interaction with the metal, as reflected by the increase in J_{SiH} for the bound Si−H from 35 Hz for η^2-SiH_4 to 50 Hz for η^2-SiH_2Ph_2. This effect fosters σ coordination over OA, as does the less basic dppe ligand set with Ph substituents, where J_{SiH} is >50 Hz. All of these J_{SiH} values are much lower than J_{SiH} for the unbound Si−H (155−194 Hz), illustrating a high degree of activation of the coordinated Si−H. The X-ray structures of Mo(CO)(SiH_2Ph_2)(depe)$_2$ and the SiH_3Ph analogue[10] have Si−H bond distances of 1.66(6) and 1.77(6) Å; hence replacement of just one Ph by less donating H lengthens d_{SiH}, which correlates with the reduction in J_{SiH} from 50 to 39 Hz. The distance for the unbound Si−H in Mo(CO)(SiH_2Ph_2)(depe)$_2$ is 1.54(6) Å and averages 1.48 Å in free silanes, showing that moderate bond elongation occurs on coordination. In Table 3, the lowest J_{SiH}, 35 Hz, is seen for the most electron-rich R = Et and the least electron-rich R′ = H (i.e., SiH_4), and the Si−H bond becomes activated toward equilibrium OA (eq 4) similar to that in eqs 6 and 7 for the organogermane systems. By comparison GeH_4 undergoes complete OA for the depe system and forms a σ complex only for the less basic dppe system. As can be seen in Table 3, germanes generally undergo OA more easily than silanes. However, neither GeH_2Ph_2 nor SiH_2Ph_2 even binds to Mo(CO)(dppe)$_2$, which does bind H_2 and less sterically encumbered silane and germanes. Because dppe is quite bulky compared to depe, it would appear that steric as well as electronic factors may be important in this system, especially for large substituents on Si/Ge such as Ph. Even monosubstituted SiH_3Ph and GeH_3Ph bind weakly to Mo(CO)(dppe)$_2$, and solid complexes cannot be isolated here (NMR evidence only).[10]

The structures of the products of reaction of the germanes with the Mo complexes are much more variable and dependent on the nature of the ligands than those of the silane system, which are in all cases η^2 σ complexes. This is especially true in solution where two or even three isomers have been found to be present in equilibrium for the Ge complexes. The seven-coordinate germyl hydride OA products show isomeric behavior in solution, which is not seen for silyl hydride complexes. In line with the bonding principles outlined above, the OA product MoH(GeH_2Ph)(CO)(depe)$_2$, **4**, results on addition of GeH_3Ph, which has only one organo substituent (eq 5). Decreasing the phosphine basicity (dppe instead of depe) on Mo gives back the σ complex **5-η^2**, which is in equilibrium with the germyl hydride, **5-oa** (eq 7). Solutions of Mo(CO)(GeH_2Ph_2)-(depe)$_2$, **3**, also show very similar equilibria, but there is evidence for a third isomer that could have proximal hydride germyl ligands and depe ligands in the same plane. It may represent an initial OA product normally not observed (never seen in the silane or H_2 systems) because rapid rearrangement presumably leads to the pentagonal bipyramid geometry with distal H and E ligands (E = germyl, silyl, H) as observed in **4** (Figure 4) as well as in **5-oa** (NMR evidence) and MoH_2(CO)-(depe)$_2$ (X-ray[12b]).

X-ray crystallography of the six-coordinate σ complexes Mo(CO)(EH_2Ph_2)(depe)$_2$ confirms the η^2-coordination mode of the E−H bond (E = Ge, Figure 2; E = Si, Figure 3). Both the germane and the silane ligands are cis to CO most likely for steric/electronic reasons, principally because these ligands are all good π acceptors and prefer to be mutually cis to avoid competing

for back-donation.[19,20] The exception is the smaller and perhaps more weakly π-accepting H_2 ligand, which binds trans to CO in $Mo(CO)(H_2)(dppe)_2$ and undergoes OA for the depe analogue, but never is observed cis to CO. As shown by calculations below, there is often little energy difference between the cis and trans isomers of models for the germane complexes and also for σ coordination versus OA, which may explain the greater variety of isomers compared to silane analogues. There is no evidence for interligand interactions[1d] between the σ ligand and the ancillary ligands in any of these complexes. Distances and angles for the GeH_2Ph_2 versus SiH_2Ph_2 complexes are compared in Table 2. The coordinated $Ge-H_{Mo}$ bond in **3** is lengthened (2.08(6) Å) versus the uncoordinated $Ge-H_{Ge}$ bond (1.49(7) Å) to a much greater extent than that for the corresponding Si−H distances in the silane analogue $Mo(CO)(SiH_2Ph_2)(depe)_2$ ($Si-H_{Mo}$ = 1.66(6) Å and $Si-H_{Si}$ = 1.54(6) Å). This nearly 0.6 Å stretching of the coordinated Ge−H bond would appear to reflect the higher degree of activation toward OA for germanes compared to their silane congeners generally observed in this system.

Importantly, it should be noted here that the structure of $Mo(CO)(\eta^2\text{-}GeH_2Ph_2)(depe)_2$, **3**, showed disorder in the position of several carbon atoms in the depe ligand which initially did not appear to be critical. However, the $Mo-H_{Mo}$ distance determined from difference maps in the X-ray structure was unreasonably long, 2.58(7) Å, especially when compared to the calculated value of 1.753 Å (see section 5.1). This X-ray distance paradoxically suggested a very weak Mo−H interaction characteristic of a weak σ complex early along the reaction coordinate toward OA and did not make sense chemically. The puzzle was resolved after a suggestion by Parkin that disorder involving a small percentage of a molecule with the germane ligand rotated approximately 180° could be producing a false position for H_{Mo}.[21] This was verified to be case, and the Ge atom was refined in two sites, with variable site occupancy factors that converged to 95.9(2)% for Ge1 and 4.1(2)% for Ge1′.

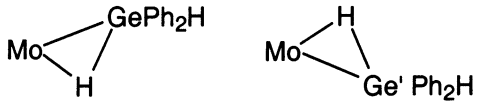

96% 4%

The lighter phenyl group carbon atoms corresponding to Ge1′ were not observed. The electron density for Ge1′ (0.041 × 32 e = 1.3 e) which was located 2.624(13) Å from Mo was thus essentially mistaken for the electron density for H_{Mo}, which had refined to be 2.58(7) Å from Mo. The H_{Mo} was located in the predominant (96%) molecule, and the $Mo-H_{Mo}$ distance now refined to be a much more reasonable 1.72(6) Å, in close agreement with the calculated value (the Ge−H and Mo−Ge distances did not change significantly). The serves as a caveat to maintaining blind faith in crystallographic data: any abnormal distances or chemically unreasonable structural features should be closely investigated for crystallographic problems such as positional disorder.

In the analogous silane complex, $Mo(CO)(SiH_2Ph_2)(depe)_2$, the Mo−H distance is longer, 2.04(2) Å, in accord with a less activated and more genuine σ ligand. However for the SiH_3Ph complex the Mo−H distance is short, 1.70(5) Å,[10] and more like that in classical hydrides, indicating that the silane is on the brink of OA, much like the germane ligand in $Mo(CO)(GeH_2Ph_2)(depe)_2$. The $Si-H_{Mo}$ = 1.77(6) Å and the uncoordinated $Si-H_{Si}$ bond distance is 1.42(6) Å; that is, the coordinated η^2-E−H bond is more elongated for the SiH_3Ph complex than for either the SiH_2Ph_2 or GeH_2Ph_2 complexes (in accord with the J_{SiH} data discussed above). The Mo−Ge distance (2.6368(7) Å) in **3** is similar to the Mo−germyl distance in the OA product **4** (2.6693(5) Å). As a result of this activation, the geometry about E in $Mo(CO)(EH_2Ph_2)(depe)_2$ becomes distorted trigonal bipyramidal and appears to approach that for an octahedral fragment where the Ph−E−Ph angle is getting close to 90° and $H_{Mo}-E-H_E$ approaches 180°. The GeH_2Ph_2 complex shows the most distortion in Ph−E−Ph, 99.15(17)°, versus 103.0(4)° in the SiH_2Ph_2 complex.

As in most other H_2 and σ complexes containing phosphine and CO ligands, the coordinated E−H bond lies approximately in the same plane as P−Mo−P rather than P−Mo−CO (dihedral angle, ϕ = 5° in **3**) to gain maximum back-donation by avoiding competing with back-donation from Mo to CO.

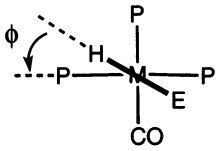

E = Si, Ge

However ϕ is much greater for E = Si (53°, and 30.5° for the SiH_3Ph analogue[10]), possibly because steric contacts, e.g., Ph rings with the other ligands, impede the electronically preferred alignment. The somewhat longer (0.07 Å) Mo−Ge bond compared to Mo−Si should place the Ph groups farther away, decreasing intramolecular interactions.

Summarizing, the ease of OA of σ bonds on the Mo complexes gives the following comparison: Ge−H > Si−H ≈ H−H ≫ C−H. This also correlates with the degree of back-donation from the metal to the σ^* orbital of the σ bond, which directly influences bond cleavage.[1] Depending on the substituent on the silane, the Si−H bond is often more difficult to cleave than the H−H bond, which coordinates to the Mo-dppe complex in η^2 fashion but undergoes OA on the more electron-rich Mo-depe complex. As shown by theoretical calculations discussed below, this relative ordering of ease of OA can be correlated with the E−H and M−E bond energies.

5. Computational Studies of Germane versus Silane Bonding and Activation

5.1. Theoretical Studies of $Mo(CO)(dhpe)_2(EH_{4-n}vin_n)$ Model Complexes. The first theoretical studies of silane coordination consisted of extended Huckel analyses of $CpMnL_2(HSiR_3)$ complexes, which demonstrated the presence of the three-center σ type interac-

(19) Butts, M. D.; Kubas, G. J.; Luo, X.-L.; Bryan J. C. *Inorg. Chem.* **1997**, *36*, 3341.
(20) Fan, M.-F.; Jia, G.; Lin, Z. *J. Am. Chem. Soc.* **1996**, *118*, 9915.
(21) Parkin, G., private communication.

Scheme 1

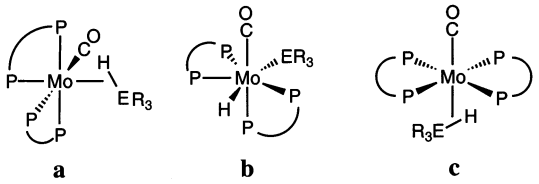

tion.[22] Subsequently ab initio calculations relevant to our system were carried out on $Mo(CO)(SiH_4)(PH_3)_4$[20] and $RuH_2(H_2)(EH_4)(PH_3)_2$ (E = Si, Ge)[23] models, which will be discussed in section 5.2. To obtain further insight into the Ge−H and Si−H activation processes, ab initio DFT calculations have been performed on $Mo(CO)(EH_{4-n}vin_n)(dhpe)_2$ model complexes (E = Si, Ge; $n = 0-3$; dhpe = $H_2PCH_2CH_2PH_2$; vin = $CH{=}CH_2$). We have attempted to remain as close as possible to the actual complexes; for example, the traditional phosphine modeling (substitution of any phosphine by PH_3) has not been used here but rather the bidentate nature of dppe and depe has been preserved by using dhpe. To model the phenyl groups bonded to Ge and Si, we have used vinyl groups. Test calculations on the monosubstituted germane and silane EH_3Ph have been carried out to calibrate the substituent modeling. Inclusion of R groups in the phosphines along with the use of a medium-sized basis set are prohibitively demanding computationally, and consequently the calculations do not allow testing the effect of phosphine basicity on the OA process. This sacrifices the scope of the work in order to obtain better reliability, but some of the conclusions obtained may be extrapolated to the dppe and depe cases at least qualitatively.

In the first stage of the calculations, three different isomers have been fully optimized without symmetry constraints for each complex (Scheme 1). For comparative purposes, the corresponding H_2 complexes, $Mo(CO)(H_2)(dhpe)_2$, have also been optimized. Isomer **a** corresponds to the structure of the synthesized germane complex, a pseudo-octahedral σ complex with the $EH_{4-n}vin_n$ occupying a single coordination site cis to the CO. Isomer **b** is the OA product, a seven-coordinate pentagonal bipyramidal structure with a P atom between the hydride and the germyl, silyl, or the other hydride ligand in the case of $MoH_2(CO)(dhpe)_2$. Isomer **c** is also a pseudo-octahedral σ complex but with the $EH_{4-n}vin_n$ or H_2 moiety trans to CO (the neutron diffraction structure of $Mo(CO)(H_2)(dppe)_2$ shows this geometry).[12c] After optimization, these structures are found to be essentially stable for all the complexes, with only one exception discussed below. The geometric parameters of the E−H−Mo moiety are listed in Table 4, and the optimized geometries of the three isomers of the $Mo(CO)(GeH_2vin_2)(dhpe)_2$ complex are depicted in Figure 9. As shown in Table 4, the optimized parameters of the Mo−E−H unit for the EH_3vin complexes differ by less than 0.02 Å from that of the EH_3Ph, supporting the validity of the substituent modeling employed.

First it must be noted that Mo−E and Mo−H distances are similar in all cases when isomers **a** and **b** are compared, while **c** behaves markedly different, with longer Mo−E and Mo−H distances. This indicates that, although there is significant E−H interaction in **a** (Ge−H distance ranges from 1.825 to 1.916 Å, while Si−H distance = 1.628−1.731 Å; cf. a Ge−H distance of ∼1.54 Å and a Si−H distance of ∼1.47 Å for the

Table 4. B3LYP Optimized Parameters of the Mo−E−H (E = Si, Ge, H) Unit and Relative Energies of a, b, and c Isomers of $Mo(CO)(L)(dhpe)_2$ Models (distances (*d*) in Å, relative energies in kcal/mol)

L	rel energy	*d*(Mo−E)	*d*(Mo−H)	*d*(E−H)
GeH_4				
a	0.0	2.693	1.742	1.916
b	1.6	2.710	1.748	4.220
c	3.7	2.860	1.844	1.687
GeH_3vin[a]				
a	0.0 (0.0)	2.701 (2.693)	1.746 (1.747)	1.897 (1.891)
b	2.9 (2.4)	2.722 (2.723)	1.749 (1.748)	4.249 (4.243)
c	3.0 (3.0)	2.848 (2.830)	1.832 (1.833)	1.701 (1.708)
GeH_2vin_2				
a	0.0	2.743	1.753	1.832
b	3.7	2.755	1.747	4.249
c	0.5	2.863	1.839	1.697
$GeHvin_3$				
a	0.0	2.766	1.752	1.825
b	6.1	2.807	1.753	4.320
c	3.1	3.044	1.877	1.645
SiH_4				
a	0.0	2.638	1.755	1.731
b	3.9	2.641	1.750	4.148
c	2.3	2.883	1.896	1.557
SiH_3vin[a]				
a	0.0 (0.0)	2.654 (2.653)	1.761 (1.760)	1.713 (1.705)
b	5.4 (4.8)	2.655 (2.654)	1.752 (1.751)	4.172 (4.168)
c	1.7 (1.8)	2.913 (2.891)	1.881 (1.877)	1.556 (1.562)
SiH_2vin_2				
a	0.9	2.737	1.774	1.654
b	7.9	2.693	1.750	4.189
c	0.0	2.949	1.891	1.552
$SiHvin_3$				
a	0.0	2.814	1.784	1.628
b	9.9	2.779	1.759	4.306
c	0.9	3.327	1.986	1.506
H_2				
a	0.6	1.868	1.878	0.842
b	5.1	1.754	1.766	3.310
c	0.0	1.966	1.933	0.804

[a] In parentheses values for the EH_3Ph complexes.

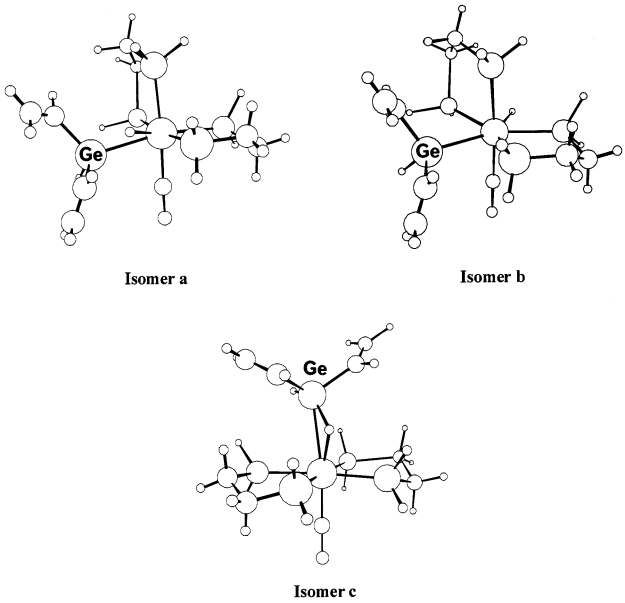

Figure 9. B3LYP optimized structures of **a**, **b**, and **c** isomers of the $Mo(CO)(GeH_2vin_2)(dhpe)_2$ model complex.

(22) Rabaa, H.; Saillard, J.-Y.; Schubert, U. *J. Organomet. Chem.* **1987**, *330*, 397.
(23) Said, R. B.; Hussein, K.; Tangour, B.; Sabo-Etienne, S.; Barthelat, J.-C. *New J. Chem.* **2003**, *27*, 1385.

optimized structures of the free germanes and silanes), these complexes have a strong hydridic character and can be described as arrested intermediates at an advanced stage of OA toward **b**. On the contrary, in **c** the much longer Mo−E and Mo−H and the shorter E−H distances are consistent with an arrested intermediate at an early stage of the OA path. This is dramatically evident for $EHvin_3$ complexes: in the $GeHvin_3$ complex, a Mo−Ge distance of 3.044 Å and a Ge−H distance of 1.645 Å are found, and in the $SiHvin_3$ complex, the Mo−Si distance is 3.327 Å and the Si−H distance (1.506 Å) is practically that of the uncoordinated silane. This phenomenon is a consequence of the silane or germane ligand being trans to a strong π-acceptor (CO), which is well known to weaken the binding and activation of a σ ligand because of reduction of M→σ* back-bonding.[1] Indeed, tertiary silane complexes of the type $Mo(CO)(SiHR_3)(dppe)_2$ could not be observed experimentally (although steric factors probably also play a role here). Because of the extremely long Mo−E distances, we can consider that the *trans*-$Mo(CO)(EH_{4-n}vin_n)(dhpe)_2$ model complexes are intermediate between an η^1 and an η^2 σ-complex where σ donation to M is the dominant interaction.

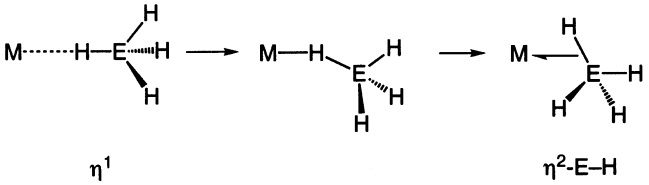

This in essence mimics an early step along the pathway for the reaction M + C−H → C−M−H derived by Crabtree[24] from structural data for agostic C−H systems using the method of Burgi and Dunitz.[25] The C−H bond initially approaches M end-on (as for incipient $M-H_2$ interaction also) and then rotates to bring the C closer to M as the C−H bond weakens and elongates. The strength of the agostic interaction and d_{MC} and d_{MH} vary greatly as for $M-H_2$ complexes, and a better yardstick is the distance from M to the point on the C−H vector where the covalent radii of C and H meet, d_{bp} in Crabtree's approach.[24]

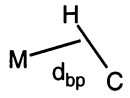

$$d_{bp} = [d_{MH}^2 + 0.0784 d_{CH}^2 - 0.28(d_{MH}^2 + d_{CH}^2 - d_{MC}^2)]^{1/2} \quad (9)$$

We have used Crabtree's approach and have calculated, using his simple relationship and our optimized geometric parameters, the value of d_{bp} for each germane and silane complex using a modified formula analogous to eq 9, where M is now Mo and C is now E. A plot of d_{bp} as a function of the E−H−Mo angle is shown in Figure 10. A clear correlation between d_{bp} and the E−H−Mo angle gives further evidence of the suggested

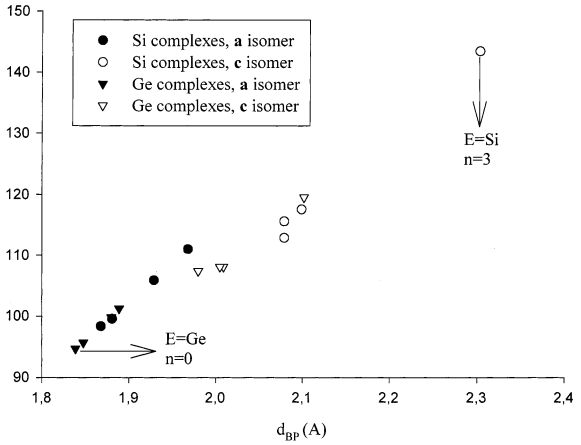

Figure 10. Plot of d_{bp} as a function of the E−H−Mo angle for **a** and **c** isomers of Ge and Si complexes.

pathway for the OA reaction. Thus, as small values of d_{bp} are related to small E−H−Mo angles and vice versa, it can be stated that $Mo(CO)(EH_{4-n}vin_n)(dhpe)_2$ model complexes range from an almost end-on η^1 coordination in the initial stages of the reaction path (more substituted Si complexes, **c** isomer) to a η^2 coordination in the more activated complexes (less substituted Ge complexes, **a** isomer). These experimental trajectories for OA of E−H and C−H[24] bonds also mirror those in theoretical studies[26,27] of CH_4 addition to model complexes such as 16e $RhCl(PH_3)$ and 14e $IrX(PH_3)_2$ (X = H, Cl).

5.2. Comparisons of Germane, Silane, and H_2 Bonding. For E = Si, a comparison can be made with a previous MP2 study in which the same three isomers were optimized for a $Mo(CO)(SiH_4)(PH_3)_4$ model.[20] Although the trends are essentially the same (longer Si−H and shorter Mo−H and Mo−Si distances for isomer **a** (cis CO) with respect to isomer **c** (trans CO) and very similar Mo−H and Mo−Si distances in **a** and **b**), there are noticeable differences between both calculations. Our Mo−Si and Mo−H distances are significantly longer than those determined by Fan et al., while the Si−H distances are shorter. Our calculations show that the $SiH_{4-n}R_n$ unit seems to be less activated in both **a** and **c**, no matter what the silane substitution pattern is. The optimized **c** isomer is in fact different than that calculated by Fan even qualitatively, since according to their calculations the Si−H bond would be considerably more elongated and would have an enhanced hydridic character that we did not find. However, their conclusions concerning structure type **a** are valid and remain unchanged by our results.

On the other hand, the progressive substitution of H by vinyl increases the Mo−E and Mo−H distances based on our calculations. Recalling that these distances are related to the degree of activation of the E−H bond (short Mo−E and Mo−H distances indicate a higher hydridic character), this fact may reflect the decreased tendency of germanes and silanes toward OA when the substituents of Ge and Si are more basic. A comparison between Si and Ge can also be made on the basis of the Mo−H distances: although in this case the differences are smaller, Ge complexes clearly have a slightly higher

(24) (a) Crabtree, R. H. *Chem. Rev.* **1985**, *85*, 245. (b) Crabtree, R. H.; Holt, E. M.; Lavin, M. E.; Morehouse, S. M. *Inorg. Chem.* **1985**, *24*, 1986.
(25) Burgi, H. B.; Dunitz, J. *Acc. Chem. Res.* **1983**, *16*, 153.
(26) Koga, N.; Morokuma, K. *Chem. Rev.* **1991**, *91*, 823.
(27) Cundari, T. R. *J. Am. Chem. Soc.* **1994**, *116*, 340.

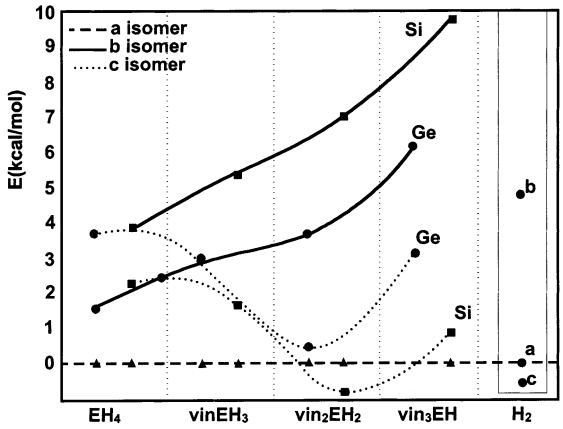

Figure 11. Relative energies of the **a**, **b**, and **c** isomers (energy of **a** = 0) for $Mo(CO)(EH_{4-n}vin_n)(dhpe)_2$ and $Mo(CO)(H_2)(dhpe)_2$.

hydridic character, as shown by shorter Mo−H. The Ge−H and Si−H distances, although not strictly comparable, show that in Ge complexes the E−H bond is more activated. For instance, in the EH_4 complexes, the Ge−H distance is almost 0.2 Å longer than the Si−H distance for isomer **a**, which is a remarkable difference even taking into account that a Ge−H bond must be slightly longer than a Si−H bond. Thus, it is obvious that Ge complexes are closer to OA products than Si complexes, as also seen from a DFT study of germane and silane activation in ruthenium complexes.[23] This study also compared GeH_4 and H_2 coordination: both ligands are better electron donors than acceptors but the Ge−H bond appears to be a better acceptor than H−H.

The relative energies of the three isomers for the entire family of complexes containing $EH_{4-n}vin_n$, depicted in Figure 11, are consistent with the aforementioned observations. In almost all cases isomer **a** is the most stable one (the only exception being the complex with SiH_2vin_2, where **c** is 0.9 kcal/mol below **a**), but **a** and **c** are often close in energy. The OA product **b** is in general not favored. Even on thermodynamic grounds an equilibrium involving **a**, **b**, and **c** is not expected except for the GeH_4 complex. This probably means that the dhpe model phosphine is not basic enough to lead to the complete breaking of E−H. However, it is reasonable to expect that for depe complexes the relative stability of **a** and **b** could be reversed for GeH_4 and perhaps for GeH_2vin_2 and SiH_4 as well. It must also be noted that the OA product is much higher in energy for Si complexes than for Ge complexes, in agreement with experimental data, and reflects the greater tendency of germanes toward full OA.

The relative energies of the isomers calculated using the actual EH_3Ph ligand are collected in Table 4 (shown in parentheses) and further confirm the validity of the substituent modeling employed. For both the Ge and Si the relative energies of the monosubstituted vinyl and phenyl σ complexes are the same. Only a difference of 0.5 kcal/mol is found between the OA products **b** with vinyl and phenyl substituents. The main effect of modeling a phenyl by a vinyl is the slight destabilization of the OA product. The substitution of H by vinyl in $EH_{4-n}vin_n$ leads to clear trends on increasing *n* from 0 to 2. First, the stability of isomer **c** with respect to **a** increases. As we will demonstrate below, isomer **a** is in a more advanced stage of OA, and thus back-donation is more important in this isomer than in **c**. The decrease in back-donation caused by the substitution of H by vinyl has a greater effect in the **a** isomers than in **c**, where there is strong competition for back-bonding by the trans CO. For GeH_2vin_2 complexes with dhpe phosphines, an equilibrium between both forms is possible (the energy difference is only 0.5 kcal/mol). Isomer **c** is more favorable for silane complexes than for germane complexes, and **a**↔**c** equilibria could take place but have not been identified experimentally.

The case of the $EHvin_3$ complexes (increasing *n* to 3) is somewhat striking, as the aforementioned trend is drastically broken because of a factor that destabilizes **c**. On the basis of the geometric parameters of the Mo−H−E unit, it has been stated that substitution of H by vinyl weakens the Mo−E bond (the Mo−E distance is significantly longer, Table 4). At the limit for $GeHvin_3$ and $SiHvin_3$, the Ge or Si is almost unbound and the Mo−H bond is not strong either (it is clearly weaker than for **a** and **b**, in which H has a strong hydridic character). Because the $EHvin_3$ is so weakly bound to Mo, this additional instability of **c** is reflected by a relative energy higher than expected. Another notable pattern concerns the OA product: progressive substitution of H by an organo group (vinyl) in the germane or silane disfavors activation toward the OA product **b**, in agreement with experimental observations in these and other systems.[2a,10,11,19]

The related $Mo(CO)(H_2)(dhpe)_2$ complexes exhibit a somewhat different behavior in both their geometric and energetic patterns. Indeed, both isomers **a** (H_2 cis to CO) and **c** (H_2 trans to CO) are true σ complexes, with calculated H−H distances of 0.842 and 0.804 Å, respectively. The neutron diffraction distance in $Mo(CO)(H_2)(dppe)_2$, which has the correctly predicted **c** geometry, is ∼0.84 Å.[12c] The short calculated H−H distance for **a** and **c** indicates that they are arrested intermediates in an early stage of OA with the H_2 weakly bonded to Mo, especially in **c**, where H_2 and CO compete for back-donation. This situation clearly differs from that found for germane complexes and, to a lesser extent, for silane complexes, where isomer **a** is more advanced toward OA. The Mo−H distances emphasize this trend: in the H_2 complexes they range from 1.868 to 1.963 Å (comparable to that for isomer **c** of $Mo(CO)(EH_{4-n}vin_n)(dhpe)_2$) but are significantly shorter in **a** and close to those of the OA product **b**. At the same time, there seems to be a correlation between the degree of the OA and the relative stability of isomers **a** and **c**. For H_2 complexes the latter isomer is more stable than the former by 0.6 kcal/mol. This difference, much smaller than that found by Fan,[20] could be traced to the different phosphine modelization and suggests that there could be an equilibrium between both isomers. In contrast, the OA product **b** lies 5.1 kcal/mol above the most stable isomer **c** and thus would not be expected to be isolated on either thermodynamic or kinetic grounds. Experimentally, for the much more basic phosphine depe, isomer **b** ($MoH_2(CO)(depe)_2$) forms as expected because increased back-donation to H_2 σ* now cleaves the H−H bond.[12b]

It is interesting to compare the position of **a** and **c** σ complexes along the OA pathway from the analysis of

Scheme 2

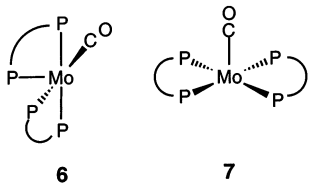

6 **7**

the bonding energies of $EH_{4-n}vin_n$ to the five-coordinate $Mo(CO)(dhpe)_2$ fragment. As an example, we have performed this analysis for the EH_2vin_2 ligands. Two square-planar pyramidal isomers of the five-coordinate transition metal fragment have been optimized (Scheme 2): in fragment **6** a phosphorus atom is occupying the apical position, while in **7** the apical position is occupied by CO. Fragment **6** is thus related to the pseudooctahedral **a** isomer of $Mo(CO)(EH_2vin_2)(dhpe)_2$ and **7** is the precursor of **c**. By using the energy difference between the optimized complexes and the sum of the energies of the optimized metal fragments and ligands, we have a simple way to estimate the bonding energies of EH_2-vin_2 to Mo. Obtaining the bonding energy for **a** implies the use of fragment **6**, and the bonding energy for **c** implies using **7**. Bonding energies of −19.7 and −12.6 kcal/mol have been obtained for the **a** and **c** isomers of the GeH_2vin_2, respectively, the values for the silane isomers being −16.9 and −11.2 kcal/mol, respectively. All the bonding energies are in the expected range for a σ complex (10−20 kcal/mol), but the EH_2vin_2 ligand forms a stronger bond with Mo in **a** compared to **c** and for E = Ge compared to E = Si. This is consistent with the geometries shown by the optimized complexes: **c** shows both longer Mo−E and Mo−H distances, and this is also reflected in the smaller bond energies. Thus the $Mo-EH_2vin_2$ bonding energy can be correlated with the ease of OA, considering that isomer **a** is in a more advanced stage of this process and that OA is more favorable for germane than for silane. The same trends hold for the entire series of $EH_{4-n}vin_n$ ligands considered in the theoretical study.

Another interesting conclusion arises from the relative energies of the five-coordinate $Mo(CO)(dhpe)_2$ fragments. The precursor complexes used to synthesize the actual $Mo(CO)(GeH_{4-n}R_n)(dppe)_2$ complexes are structurally related to fragment **7** with the CO in the apical position of the pentagonal bipyramid. Calculations indicate that this optimized fragment is 6.7 kcal/mol more stable than **6**, which means that in the first stage of the process $EH_{4-n}R_n$ might coordinate to the vacant site trans to CO, leading to **c**, which would then be kinetically favored over **a**. The fact that the thermodynamically unstable **c** is not unequivocally detected even as an intermediate means that the interconversion process between both isomers is fast, which is not surprising because the small $Mo-EH_{4-n}R_n$ bonding energy facilitates dissociation. NMR spectra of the germane complexes do show signals for unidentified equilibrium species such as **3-x** that might be due to a **c**-type isomer.

5.3. Thermodynamic Approach to the Oxidative Addition Process. The reaction coordinate for activation of the E−H bond toward OA can also be analyzed in terms of fragments and bonding energies by means of the thermodynamic cycle depicted in Scheme 3. We

Scheme 3

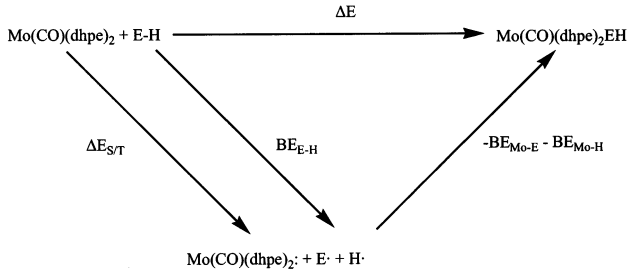

Table 5. Energetic Analysis of the Oxidative Addition Process from the Optimized $Mo(CO)(dhpe)_2$ and $EH_{4-n}vin_n$ (E = Ge, Si, n = 0−3; E = C, n = 0) or H_2 Fragments to Obtain the Oxidative Addition Product Isomer b (all energies in kcal/mol)

	ΔE	BE_{E-H}
$MoH(GeH_3)(CO)(dhpe)_2$	−19.9	89.0
$MoH(GeH_2vin)(CO)(dhpe)_2$	−18.6	87.6
$MoH(GeHvin_2)(CO)(dhpe)_2$	−16.0	87.7
$MoH(Gevin_3)(CO)(dhpe)_2$	−13.2	89.2
$MoH(SiH_3)(CO)(dhpe)_2$	−15.0	96.2
$MoH(SiH_2vin)(CO)(dhpe)_2$	−13.4	94.5
$MoH(SiHvin_2)(CO)(dhpe)_2$	−9.9	94.3
$MoH(Sivin_3)(CO)(dhpe)_2$	−6.0	94.6
$MoH_2(CO)(dhpe)_2$	−14.4	111.7
$MoH(CH_3)(CO)(dhpe)_2$	+14.6	113.5

have already analyzed the ability of transition metal fragments to break the H−H bond using this cycle,[28,29] and now we want to extend this to other σ bonds. According to this analysis, the reaction from the $Mo(CO)(dppe)_2$ and $EH_{4-n}vin_n$ fragments to give the oxidative addition product can be visualized as a multistep process, and the ΔE for the OA reaction can be broken down into some easily understandable terms that allow comparison between the different σ bonds involved. The ΔE term gives an indication of the thermodynamic viability of the OA process and can be easily calculated for all the complexes of the family as the difference between the energy of isomer **b** of $Mo(CO)(EH_{4-n}vin_n)$-$(dhpe)_2$ and the energies of the $Mo(CO)(dhpe)_2$ and $EH_{4-n}vin_n$ fragments. To compare the OA of silanes and germanes with the well-known case of H_2, a similar **b**-like isomer of $MoH_2(CO)(dhpe)_2$ has also been included in the series. We have extended the comparison to the C−H bond, considering the simplest CH_4 case. The results are listed in Table 5. As expected, more negative ΔE's are obtained for Ge than for Si, indicating that the OA process is more favorable for Ge than for Si. Moreover, the absolute values of the ΔE term decrease when H atoms are replaced by vinyls, giving further proof that this substitution disfavors OA. OA of H_2 falls between that for Si−H and Ge−H bonds: it is more favorable than the majority of Si cases, but it is unfavorable compared to all the Ge cases except for the more substituted $GeHvin_3$. The behavior of the C−H bond toward the OA is strikingly different: the oxidative addition process turns out to be a highly endothermic reaction on this molybdenum model complex.

The overall ΔE between the fragments and the final product can be decomposed in several terms. In a first

(28) Tomàs, J.; Lledós, A.; Jean, Y. *Organometallics* **1998**, *17*, 4932.
(29) Lesnard, H.; Demachy, I.; Jean, Y.; Lledós, A. *Chem. Commun.* **2003**, 850.

stage, the E−H bond is broken (requiring an energy equal to BE_{E-H}) and the metal fragment is promoted to a triplet state ($\Delta E_{S/T}$) in which there are two unpaired electrons in the convenient molecular orbital ready to form two covalent bonds. When the three fragments so obtained are put together (which is related to the M−Eand M−H bonding energies), the final OA product is reached (eq 9).

$$\Delta E = \Delta E_{S/T} + BE_{E-H} - BE_{Mo-E} - BE_{Mo-H} \quad (9)$$

$\Delta E_{S/T}$ for the $Mo(CO)(dhpe)_2$ fragment does not vary because the metal fragment is not changed. The Mo−H bonding energy may be considered essentially unchanged for our purposes, an assumption consistent with the similarity of the Mo−H distances found in the entire family of complexes. If we group these two terms into a constant *K*, a simplified eq 10 is obtained.

$$\Delta E = BE_{E-H} - BE_{Mo-E} + K \quad (10)$$

Thus, the ease of OA (ΔE) is explicitly related to the E−H and M−E bonding energies: the process will be favored by a large M−E bonding energy and a small E−H bonding energy.[28,29] DFT methods have been very recently used to study bond energy M−C/C−H correlations.[30]

In the previous work[28,29] very accurate CCSD(T) energy values were calculated for all the terms of the cycle. The size of the systems considered in the present study prevents us from using this methodology, and only B3LYP energy values have been obtained. However, as we will show later on, these values can be considered a good approximation for discussion purposes. The energy difference between the optimized geometries of the triplet and singlet states of the five-coordinate $Mo(CO)(dhpe)_2$ fragment **6** ($\Delta E_{S/T}$) is 18.7 kcal/mol. This DFT value is in reasonable agreement with that obtained at the CCSD(T) level for the related $Mo(PH_3)_5$ fragment (23.6 kcal/mol).[28] To compare the behavior of the different E−H bonds toward oxidative addition, we will consider the simplest, nonsubstituted EH_4 molecules. To obtain the M−E bonding energies, the $Mo(SiH_3)_2(CO)(dhpe)_2$, $Mo(GeH_3)_2(CO)(dhpe)_2$, $MoH_2(CO)(dhpe)_2$, and $Mo(CH_3)_2(CO)(dhpe)_2$ complexes have been optimized starting from a geometry similar to that of the **b** isomer of the previous complexes (i.e., a phosphine between the two SiH_3, GeH_3, H, or CH_3 ligands, ensuring that OA is complete).

$$Mo(CO)(dhpe)_2\,(\textbf{6-triplet}) + 2EH_3^{\bullet} \rightarrow Mo(EH_3)_2(CO)(dhpe)_2\,(\textbf{b}\text{ isomer}) \quad (11)$$

The energy of the reaction in eq 11 is approximately 2 times the Mo−E bond energy ($-2 \times BE_{Mo-E}$). In this way bond energies of 51.5 kcal/mol (Mo−Ge), 54.3 kcal/mol (Mo−Si), 72.0 kcal/mol (Mo−H), and 43.6 kcal/mol (Mo−C) have been obtained. The computed Mo−H and $Mo-CH_3$ bond energies are in the range of experimental values. Bond enthalpies of 61.7 ± 1.9 and 39.8 ± 1.9 kcal/mol have been reported for the Mo−H and Mo−C bonds of Cp_2MoR_2 (R = H, Me) complexes and 67.7 ± 1.4 and 48.7 ± 1.9 kcal/mol for $CpMo(CO)_3R$ (R = H, Me).[31] Moreover, our difference between the BE_{Mo-H} and BE_{Mo-C} (28.4 kcal/mol) compares favorably with the difference between the mean experimental values (21.8 kcal/mol).[31] An Mo−H bond energy of 75.0 kcal/mol was obtained at the CCSD(T) level for $MoH_2(PH_3)_5$.[28] The comparison of our B3LYP Mo−E bond energies with the previous values agrees with a good estimation of the bond energies.

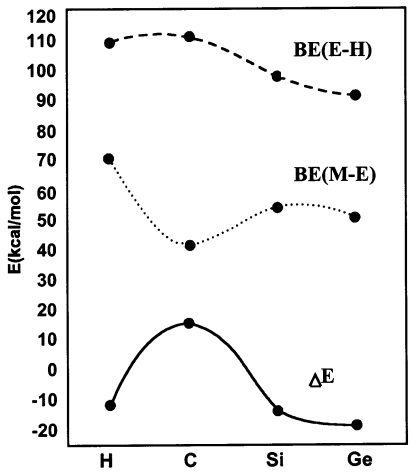

Figure 12. Plot of the calculated BE_{Mo-E}, BE_{E-H}, and ΔE values.

The calculated BE_{Mo-E}, BE_{E-H}, and ΔE are plotted in Figure 12. A main feature arising from these calculations is that the Mo−H bond is significantly stronger than Mo−Si and Mo−Ge bonds. However, the only slightly higher energy (2.8 kcal/mol) of the Mo−Si bond versus Mo−Ge indicates that the term ruling the thermodynamics of the OA process for silanes and germanes might be the E−H bond energy. These bond energies, calculated as the energy difference between the EH_4 optimized compounds and the energies of the EH_3 and H doublet fragments, are listed in the last column of Table 5 and clearly indicate that the Si−H bond is about 7 kcal/mol stronger than the Ge−H bond. Recalling that the ease of the entire OA process is a balance between the E−H bond energy and Mo−E bond energy (see eq 10), it can be concluded that the factor that makes OA of Ge−H easier than that for Si−H is the relative weakness of the Ge−H bond, despite the fact that the Mo−Ge bond is also weaker. As the E−H bond energies are nearly unaffected by the substitution, the main factor responsible for the decreasing exothermicity of the OA with the increasing of the substitution must lie on the lowering of the $Mo-EH_{3-n}R_n$ bond energy when increasing *n*.

The competition between both factors is also seen for OA of H_2, for which although the Mo−H bond energy is much higher than the Mo−Si and Mo−Ge bond energies, the H−H bond is also significantly stronger than the Si−H and Ge−H bonds (a BE of 111.7 kcal/mol is calculated for the H−H bond at the B3LYP level). On the whole, the ease of OA of H_2 is between that of germanes and silanes (ΔE in Table 5). From the curves in Figure 12 the anomalous behavior of the M−C bond and its responsibility for the highly endothermic ΔE for the OA of the C−H bond can be clearly appreciated. The

(30) Clot, E.; Besora, M.; Maseras, F.; Mégret, C.; Eisenstein, O.; Oelckers, B.; Perutz, R. N. *Chem. Commun.* **2003**, 490.

(31) Martinho Simoes, J. A.; Beauchamp, J. L. *Chem. Rev.* **1990**, *90*, 629, and references therein.

BE_{E-H} and BE_{Mo-E} curves are almost parallel, with the exception of the BE_{Mo-C} point. The Mo−C bond energy should be more than 25 kcal/mol higher to keep the two curves parallel. It was already pointed out that the OA in alkanes is much more difficult because the loss of the high C−H bond energy (comparable to or greater than that for H−H) is not as well compensated for since M−C bonds in L_nM−alkyl complexes are weaker than the corresponding L_nM−H bonds by 15−25 kcal/mol.[32] This trend is very well reproduced by our calculations.

As a last point, an extrapolation of our results to other metal fragments with different phosphines can be qualitatively made using the $\Delta E_{S/T}$ term. In previous articles[28,29] it has been suggested that the terms associated with the bonding energies are mainly dependent on the identity of M and the bonded atom, while the $\Delta E_{S/T}$ term is related to the coordination environment of the metal fragment. In this way, a smaller $\Delta E_{S/T}$ term makes OA easier because basic ligands tend to reduce the energy gap between the singlet and the triplet states of the metal fragment. For this reason, more basic phosphines (for instance, depe instead of dhpe or dppe) are expected to favor the OA process, and indeed this is the case.

6. Summary and Conclusions

Reaction of GeH_4 and organogermanes $GeH_{4-n}Ph_n$ with $Mo(CO)(PP)_2$ (PP = diphosphine) produces germane σ complexes, $Mo(CO)(\eta^2\text{-}GeH_{4-n}Ph_n)(PP)_2$ (n = 0−2), including the first examples of a GeH_4 complex and a crystal structure of a monometallic η^2-Ge−H σ complex. η^2-Ge−H coordination as well as activation of Ge−H bonds toward OA has been established to be similar to that for silane σ complexes such as $Mo(CO)(SiH_{4-n}Ph_n)(PP)_2$ except that the Ge−H bond undergoes OA more easily to seven-coordinate $MoH(SiH_{3-n}Ph_n)(CO)(depe)_2$. The latter germyl hydrides as well as germane σ complexes generally show isomeric forms in solution not observed in analogous silane systems. When the more electron-rich phosphine depe (depe = $Et_2PC_2H_4PEt_2$) is used, oxidative addition (OA) products $MoH(GeH_3)(CO)(depe)_2$ and $MoH(GeH_2Ph)(CO)(depe)_2$ are isolated (NMR and X-ray evidence). However, when the secondary organogermane GeH_2Ph_2 is used in the depe system, the η^2-complex $Mo(CO)(\eta^2\text{-}GeH_2Ph_2)(depe)_2$ is obtained. The latter was found to be in tautomeric equilibrium with its OA product as well as a third isomer of unknown structure. Comparisons of structure, bonding, and activation to OA were made to the analogous silane complexes, e.g., $Mo(CO)(\eta^2\text{-}SiH_2Ph_2)(depe)_2$, the X-ray structure for which is also reported.

To obtain further insight into Ge−H versus Si−H activation, ab initio DFT calculations have been performed on $Mo(CO)(EH_{4-n}vin_n)(dhpe)_2$ model complexes (E = Si, Ge; n = 0−3; dhpe = $H_2PCH_2CH_2PH_2$) and also the analogous H_2 complex. Vinyl groups (vin = CH=CH_2) were used to model the phenyl substituents on the germanes and silanes. Test calculations with the monosubstituted EH_3Ph ligands validate the substituent modeling. Three different isomers were optimized for each complex: isomer **a**, corresponding to the octahedral structure of the synthesized silane and germane complexes with the $EH_{4-n}vin_n$ cis to the CO; isomer **b**, the seven-coordinate OA product; and isomer **c** with the σ ligand trans to CO. The Mo−E and Mo−H distances are similar in all cases when isomers **a** and **b** are compared, while **c** behaves markedly different, with longer Mo−E and Mo−H distances. This indicates that, although there is significant E−H interaction in **a**, these complexes have a strong hydridic character and can be described as arrested intermediates at an advanced stage of OA toward **b**. In contrast, for *trans*-$Mo(CO)(EH_{4-n}vin_n)(dhpe)_2$ (**c**), the much longer Mo−E and Mo−H and the shorter E−H distances are consistent with an arrested intermediate at an early stage of OA, intermediate between an η^1 and an η^2 σ complex. The reaction coordinate for activation of the E−H bond toward OA was also analyzed in terms of fragments and bonding energies. Because the ease of the whole OA process is a balance between the E−H bonding energy and Mo−E bonding energy, it was concluded that the factor that makes OA of the Ge−H bond easier than that for Si−H is the relative weakness of the Ge−H bond, despite the fact that the Mo−Ge bond is also weaker. This competition between both factors is also seen for OA of H_2 on $Mo(CO)(dhpe)_2$. Although the Mo−H bonding energy is much higher than the Mo−E bonding energies, the H−H bond is also significantly stronger than the E−H bonds, and the ease of OA of H_2 lies between that of germanes and silanes. Similar calculations for the OA of C−H using the CH_4 substrate confirms that for alkanes OA is more difficult because the loss of the high C−H bond energy (comparable to or greater than that for H−H) is not as well compensated for since M−C bonds in L_nM−alkyl complexes are weaker than the corresponding L_nM−H bonds by 15−25 kcal/mol.[32]

7. Experimental Section

General Procedures. NMR spectra were measured on a Varian UNITY series 300 MHz spectrometer. FT-IR spectra were obtained either on a BioRad FTS-40 or on a Nicolet Magna 750 spectrometer. Solvents were dried either by distillation from Na/benzophenone (Et_2O, hexanes) or by elution from columns of activated alumina and BTS catalyst according to the procedure describe by Grubbs.[33] NMR solvents were dried over either CaH_2 or P_2O_5 and vacuum transferred before use. ^1H NMR spectra were referenced to either $CHDCl_2$ or TMS, and ^{31}P NMR spectra were referenced to H_3PO_3. All manipulations and reactions with air-sensitive compounds were carried out either in a Vacuum Atmospheres He drybox or under Ar using standard Schlenk techniques. All reactions were carried out at atmospheric pressure, which is 580 Torr at Los Alamos (elevation = 7300 ft) unless otherwise noted. Elemental analyses were performed in-house. All phosphines were purchased from Strem Chemicals and used as supplied. GeH_4 and organogermanes were purchased from Matheson Gas Products and Gelest, Inc., respectively. $Mo(CO)(dppe)_2$,[13] $Mo(CO)(^iBu_2PC_2H_4P^iBu_2)_2$,[14] and $[Mo(CO)(depe)_2]_2(\mu\text{-}N_2)$[14] were prepared according to published procedures.

Preparation of $Mo(CO)(\eta^2\text{-}GeH_4)(dppe)_2$, 1. Approximately 1 equiv of GeH_4 (estimated using the ideal gas law and a 57 mL bulb) was condensed onto a degassed and frozen

(32) Labinger, J. A.; Bercaw, J. E. *Organometallics* **1988**, *7*, 926, and references therein.

(33) Pangborn, A. B.; Giardellow, M. A.; Grubbs, R. H.; Rosen, R. K.; Timmers, F. J. *Organometallics* **1996**, *15*, 1518−1520.

solution of $Mo(CO)(dppe)_2$ (0.036 g, 0.039 mmol) in benzene (5 mL). As the mixture warmed to room temperature, a yellow solution and pale yellow solid formed in the reaction flask. The reaction vessel was taken into the drybox and the solution pipetted off. The solid was washed once with toluene (5 mL) and twice with hexanes (5 mL) to provide 0.0193 g of $Mo(CO)(\eta^2\text{-}GeH_4)(dppe)_2$ as a pale yellow powder (49% yield). Anal. Calcd for $C_{53}H_{52}GeOP_4Mo$: C, 63.82; H, 5.25. Found: C, 63.97; H, 5.47. IR (Nujol, cm^{-1}): 1969, 1938, 1922 (ν_{Ge-H}), 1795 (ν_{CO}), 1756 ($\nu_{Mo-H-Ge}$). ^1H NMR (THF-d_8): 4.4−5.5 (br, m, unbound GeH_3), −5.90 (br, m, Mo−H−*Ge*).

Preparation of $MoH(GeH_3)(CO)(depe)_2$, 2. Approximately 2 equiv of GeH_4 (estimated using the ideal gas law and a 57 mL bulb) was condensed onto a degassed and frozen solution of $\{Mo(CO)(depe)_2\}_2(\mu\text{-}N_2)$ (0.0352 g, 0.0639 mmol) in hexanes (5 mL). **2** was isolated as above as a lemon-yellow solid. Anal. Calcd for $C_{21}H_{52}GeOP_4Mo$: C, 41.14; H, 8.55. Found: C, 41.17; H, 8.52. IR (Nujol, cm^{-1}): 1928, 1887, 1857 (ν_{Ge-H}), 1756 (ν_{CO}), 1728 (ν_{Mo-H}). NMR showed two isomeric species were present in solution. Isomer **2A**: ^1H NMR (C_7D_8, −80 °C): 3.27 (br s, GeH_3), 0.2−2.8 (br, depe), −7.85 (m, GeHMo). $^{31}P\{^1H\}$ NMR (C_7D_8, −80 °C): 84.4 (1P), 62.7 (2P), 34.5 (1P). Isomer **2B**: ^1H NMR (C_7D_8, −80 °C): 2.56 (s, GeH_3), 0.2−2.8 (br, depe), −7.59 (quintet, J_{HP} = 41.3 Hz, GeHMo). $^{31}P\{^1H\}$ NMR (C_7D_8, −80 °C): 66.3 (br) Integrated ratio of **2A** to **2B** signals (−80 °C) = 4.8:1.

Preparation of $Mo(CO)(\eta^2\text{-}GeH_2Ph_2)(depe)_2$, 3. GeH_2Ph_2 (0.024 g, 0.11 mmol) was added from a 10 μL syringe to a solution of $[Mo(CO)(depe)_2]_2(\mu\text{-}N_2)$ (0.053 g, 0.048 mmol) in hexanes (5 mL), resulting in a color change from red to orange and evolution of N_2. The solution was slowly evaporated down to about one-half the volume and then stored at room temperature for 3 days, after which time yellow block-shaped crystals had formed, which were suitable for an X-ray diffraction study. The solution was pipetted off the crystals in the drybox, and the crystals were washed with 3 mL of cold hexanes and dried in vacuo to provide 0.044 g of $Mo(CO)(\eta^2\text{-}GeH_2Ph_2)(depe)_2$ (59% yield). MW = 765.28. Anal. Calcd for $C_{33}H_{60}GeOP_4Mo$: C, 51.79; H, 7.90. Found: C, 51.66; H, 7.93. IR (Nujol, cm^{-1}): 1838 (ν_{Ge-H}), 1780 (ν_{CO}), 1757 ($\nu_{Mo-H-Ge}$). NMR showed three isomeric species were present in solution. Isomer **3-oa**: ^1H NMR (C_7D_8, −80 °C): 8.35 (br s, 2H, Ph), 7.0−7.43 (m, 4H, Ph), 5.39 (m, Ge*H*), 0.3−2.6 (m, depe), −8.48 (m, Ge*H*Mo). $^{31}P\{^1H\}$ NMR (C_7D_8, −80 °C): 91.9, 61.8, 60.0, 35.7. Isomer **3-η^2**: ^1H NMR (C_7D_8, −80 °C): 8.06 (d, J_{HH} = 6.6 Hz, 2H, Ph), 7.0−7.43 (m, 4H, Ph), 5.87 (m, Ge*H*), 0.3−2.6 (m, depe), −6.30 (m, GeH_{Mo}). $^{31}P\{^1H\}$ NMR (C_7D_8, −80 °C): 38.0, 49.4, 56.1, 68.8. Isomer **3-x**: ^1H NMR (C_7D_8, −80 °C): 7.98 (d, J_{HH} = 6.6 Hz, 2H, Ph), 7.0−7.43 (m, 4H, Ph), 5.09 (m, Ge*H*), 0.3−2.6 (m, depe), −6.82 (m, Ge*H*Mo). $^{31}P\{^1H\}$ NMR (C_7D_8, −80 °C): 84.6, 51.3.

Preparation of $MoH(GeH_2Ph)(CO)(depe)_2$, 4. GeH_3Ph (0.019 g, 0.12 mmol) was added from a 10 μL syringe to a solution of $[Mo(CO)(depe)_2]_2(\mu\text{-}N_2)$ (0.061 g, 0.055 mmol) in hexanes (3 mL). The reaction mixture instantly turned from red to yellow, and a small amount of bubbling was observed due to the release of N_2. The solution was stored at −30 °C for 24 h, after which time pale yellow prism-shaped crystals had formed, which were suitable for an X-ray diffraction study. The solution was pipetted off the crystals in the drybox, and the crystals were washed with 3 mL of cold hexanes and dried in vacuo to provide 0.062 g of $MoH(GeH_2Ph)(CO)(depe)_2$ (82% yield). MW = 689.19. Anal. Calcd for $C_{27}H_{56}GeOP_4Mo$: C, 47.06; H, 8.19. Found: C, 46.74; H, 8.08. IR (Nujol, cm^{-1}): 1872, 1856 (ν_{Ge-H}), 1759 (ν_{CO}), 1720 (ν_{Mo-H}). NMR showed two isomeric species were present in solution. Isomer **4A** (major): ^1H NMR (C_7D_8, −80 °C): 8.5 (br s, 2H, Ph), 7.0−7.5 (m, 4H, Ph), 4.45 (m, Ge*H*), 0.3−2.6 (m, depe), −7.75 (m, Ge*H*Mo). $^{31}P\{^1H\}$ NMR (C_7D_8, −80 °C): 86.5, 62.6, 61.8, 32.5. Isomer **4B** (minor): ^1H NMR (C_7D_8, RT): 7.72 (d, J_{HH} = 6.9 Hz, Ph), 6.9−7.4 (m, Ph), 3.93 (br s, GeH), 0.2−2.6 (m, depe), −7.52 (quintet, J_{HP} = 42.1 Hz, Ge*H*Mo). $^{31}P\{^1H\}$ NMR (C_7D_8, RT): 65.7 (br).

Preparation of $Mo(CO)(dppe)_2(\eta^2\text{-}GeH_3Ph)$, 5. GeH_3Ph (0.010 g, 0.066 mmol) was added via a 10 μL syringe to a solution of $Mo(dppe)_2(CO)$ (0.056 g, 0.061 mmol) in toluene (3 mL). Within 5 min, the color of the reaction mixture changed from black to dark orange (completely soluble). A solid product could not be isolated, but solution NMR showed the presence of two isomers. Isomer **5-η^2** (σ complex): ^1H NMR (C_7D_8, −80 °C) 8.2−6.0 (br m, 2H, Ph), 4.9 (m, GeH_2), 2.0−2.8 (br m, dppe), −5.06 (br, Ge*H*Mo). $^{31}P\{^1H\}$ NMR (C_7D_8, −80 °C): 75.6, 63.4, 59.7, 47.1. Isomer **5-oa** (germyl hydride): ^1H NMR (C_7D_8, −80 °C): 8.2−6.0 (br m, Ph), 4.59 (br, GeH_2), 2.0−2.8 (br m, dppe), −5.25 (br, Ge*H*Mo). $^{31}P\{^1H\}$ NMR (C_7D_8, −80 °C): 85.3, 65.8, 61.8, 40.9. Ratio of **5-η^2** to **5-oa** at −80 °C = 1.5:1.

Preparation of $Mo(CO)(\eta^2\text{-}SiH_4)(depe)_2$ and $MoH(SiH_3)(CO)(depe)_2$. Approximately 0.652 mmol of SiH_4 gas was condensed onto a frozen solution of $[Mo(CO)(depe)_2]_2(\mu\text{-}N_2)$ (0.359 g, 0.326 mmol) in 3 mL of toluene. The mixture was warmed to room temperature and evaporated in vacuo to dryness. The residue was triturated with 20 mL of hexane. Chilling of the mixture at −38 °C in a freezer for 2 h followed by filtration gave $Mo(CO)(\eta^2\text{-}SiH_4)(depe)_2$ as a lemon-yellow solid (219 mg, 59% yield). Anal. Calcd for $C_{21}H_{52}MoOP_4Si$: C, 44.36; H, 9.22. Found: C, 44.24; H, 9.14. IR (Nujol, cm^{-1}): ν(Si−H) 2047, 1995, 1972; ν(CO) 1775; ν(Mo−H−Si) 1732. In solution the compound exists as an equilibrium mixture of two tautomers, i.e., the η^2-SiH_4 σ complex Mo(η^2-SiH_4)(CO)$(depe)_2$ (η^2) and the hydridosilyl tautomer $MoH(SiH_3)(CO)(depe)_2$ (*OA*). $^1H\{^{31}P\}$ NMR ($C_6D_5CD_3$, 268 K): δ 4.56 (s, $^1J_{SiH}$ = 164 Hz, SiH_3, η^2), 3.48 (s, $^1J_{SiH}$ = 143 Hz, SiH_3, *OA*), 0.5−2.0 (m, PC_2H_4P, C_2H_5), −7.57 (s, MoH, *OA*), −8.23 (s, J_{SiH} = 35 Hz, Mo(η^2-H−Si), η^2). $^{31}P\{^1H\}$ NMR ($C_6D_5CD_3$, 238 K): δ 83.3 (m, 1 P, *OA*), 67.4 (m, 1 P, η^2), 63.9 (m, 1 P, *OA*), 63.4 (m, 1 P, *OA*), 53.1 (m, 1 P, η^2), 46.4 (m, 1 P, η^2), 39.1 (m, 1 P, η^2), 35.2 (m, 1 P, *OA*).

Preparation of $Mo(CO)(\eta^2\text{-}SiH_2Ph_2)(depe)_2$. $[Mo(CO)(depe)_2]_2(\mu\text{-}N_2)$ (50.0 mg, 0.0454 mmol) and SiH_2Ph_2 (16.7 mg, 0.0908 mmol) were reacted in 2 mL of Et_2O for 5 min. The mixture was evaporated in vacuo to dryness. The residue was triturated with 10 mL of hexane. Chilling of the mixture at −38 °C in a freezer for 2 h followed by filtration gave $Mo(CO)(\eta^2\text{-}SiH_2Ph_2)(depe)_2$ as a lemon-yellow solid (41 mg, 61% yield). Anal. Calcd for $C_{33}H_{60}MoOP_4Si$: C, 54.99; H, 8.39. Found: C, 54.61; H, 8.24. IR (Nujol, cm^{-1}): ν(Si−H) 2010; ν(CO) 1792; ν(Mo−H−Si) 1752. $^1H\{^{31}P\}$ NMR (C_6D_6, 298 K): δ 7.1−8.2 (m, 10H, Ph), 6.78 (d, J_{HH} = 8.2 Hz, $^1J_{SiH}$ = 172 Hz, 1H, Si−H), 0.6−2.2 (m, 48H, PC_2H_4P, C_2H_5), −7.57 (d, J_{HH} = 8.1 Hz, J_{SiH} = 50.6 Hz, 1H, Mo(η^2-H−Si)). $^{31}P\{1H\}$ NMR (C_6D_6, 298 K): δ 60.5 (ddd, $^2J_{PP}$ = 67.4, 23.7, and 19.1 Hz, 1 P), 54.2 (ddd, $^2J_{PP}$ = 68.0, 29.2, and 9.2 Hz, 1 P), 47.5 (ddd, $^2J_{PP}$ = 28.6, 25.4, and 18.7 Hz, 1 P), 34.5 (td, $^2J_{PP}$ = 48.6 and 9.5 Hz, 1 P).

Crystals of $Mo(CO)(\eta^2\text{-}SiH_2Ph_2)(depe)_2$ suitable for X-ray diffraction measurements were grown from Et_2O/hexane.

Thermodynamic Study of SiH_2Ph_2 Binding to $Mo(CO)(^iBu_2PC_2H_4P^iBu_2)_2$. $Mo(CO)(^iBu_2PC_2H_4P^iBu_2)_2$ (40.0 mg, 0.0525 mmol) and SiH_2Ph_2 (9.7 μL, 0.0525 mmol) were dissolved in 0.59 mL of $C_6D_5CD_3$. Both $^1H\{^{31}P\}$ and $^{31}P\{^1H\}$ NMR spectra of the resulting solution reveal that the η^2-silane complex $Mo(CO)(\eta^2\text{-}SiH_2Ph_2)(^iBu_2PC_2H_4P^iBu_2)_2$ is formed in equilibrium with the unreacted $Mo(CO)(^iBu_2PC_2H_4P^iBu_2)_2$ and SiH_2Ph_2. $^1H\{^{31}P\}$ NMR ($C_6D_5CD_3$, 298 K): δ 7.1−8.3 (m, Ph), 6.72 (d, J_{HH} = 7.5 Hz, $^1J_{SiH}$ = 168 Hz, unbound Si−H of bound SiH_2Ph_2), 5.07 (s, $^1J_{SiH}$ = 198 Hz, free SiH_2Ph_2), 0.4−2.4 (m, $^iBu_2PC_2H_4P^iBu_2$), −7.48 (d, J_{HH} = 7.5 Hz, J_{SiH} = 49 Hz, Mo(η^2-*H*-Si)). $^{31}P\{^1H\}$ NMR ($C_6D_5CD_3$, 298 K): one peak at δ 65.5 for unreacted $Mo(CO)(^iBu_2PC_2H_4P^iBu_2)_2$ and four peaks at δ 61.9 (ddd, $^2J_{PP}$ = 66.4, 22.9, and 18.8 Hz), 52.3 (ddd, $^2J_{PP}$ = 66.4, 32.4, and 8.9 Hz), 49.6 (ddd, $^2J_{PP}$ = 32.2, 22.9, and 18.4 Hz), 32.3 (td, $^2J_{PP}$ = 22.9 and 8.9 Hz). The equilibrium constants (K_{eq}) for eq 8 at various temperatures were measured from

$^{31}P\{^1H\}$ NMR integration: 278 K, 20.3; 288 K, 12.2; 298 K, 5.2; 308 K, 2.5; 318 K, 1.2; 328, 0.65; 338 K, 0.37. Below 278 K, the K_{eq} cannot be determined due to the partial precipitation of $Mo(\eta^2\text{-}Ph_2SiH_2)(CO)(^iBu_2PC_2H_4P^iBu_2)_2$. The plot of ln K_{eq} versus $1/T$ is linear and gives the following thermodynamic parameters: $\Delta H = -12.8 \pm 1.2$ kcal mol^{-1} and $\Delta S = -40 \pm 4$ cal mol^{-1} K^{-1}.

Computational Details. Calculations were performed using the Gaussian98 series of programs.[34] Geometry optimizations were carried out using the density functional theory (DFT)[35] with the B3LYP functional.[36] A quasi-relativistic effective core potential operator was used to represent the innermost electrons of the Mo, Ge, and Si atoms.[37] The basis set for the molybdenum atom was that associated with the pseudopotential with a standard valence double-ζ LANL2DZ contraction.[34] For Si and Ge, the standard basis associated with the pseudopotential was supplemented with single unscaled d polarization functions with exponents 0.282 and 0.230, respectively.[38] The 6-31G(d) basis set was used for the phosphorus atoms and for the carbon atom of the methyl group.[39] Hydrogens directly attached to the Ge, Si, C(Me), or Mo were described using a 6-31G(p) basis set.[39] The rest of the atoms were described using a 6-31G basis set.[39]

X-ray Crystallographic Analyses. A yellow, parallelepiped-shaped plate of $Mo(CO)(depe)_2(\eta^2\text{-}GeH_2Ph_2)$, **3**, was attached to a glass fiber using epoxy. The crystal was then placed on a Bruker P4/CCD/PC diffractometer. The data were collected using a sealed, graphite-monochromatized Mo Kα X-ray source. The lattice was determined using 183 reflections. A hemisphere of data was collected using a combination of φ and ω scans, with 30 s frame exposures and 0.3° frame widths. Data collection and initial indexing and cell refinement were handled using SMART[40] software. Frame integration and final cell parameter calculations were carried out using SAINT[41] software. The final cell parameters were determined using a least-squares fit to 6597 reflections. The data were corrected for absorption using the numerical option in XPREP (SHELXTL PC[42]). Decay of reflection intensity was not observed. The structure was solved in space group $P2_1/c$ using Patterson and difference Fourier techniques. The initial solution revealed the molybdenum, germanium, phosphorus, and the majority of all carbon atom positions. The two hydrogen atoms bonded to the germanium were located on the second difference map and were refined with their isotropic temperature factors set to 0.08 Å^2. The remaining atomic positions were determined from subsequent Fourier synthesis. The depe and phenyl hydrogen atom positions were fixed (C−H = 0.96 Å for methyl, 0.97 Å for methylene, and 0.93 Å for aromatic) using the HFIX command in SHELXTL PC.[42] The hydrogen atoms were refined using a riding model, with their isotropic temperature factors set to 1.2 (methylene, aromatic) or 1.5 (methyl) times the equivalent isotropic U of the carbon atom they were bound to. The $GePh_2H_2$ ligand and several carbon atoms in the depe ligand were disordered. The ethyl carbon atom positions were refined as two one-half occupancy sites (primed and unprimed). The germanium atom was refined in two sites, with variable site occupancy factors. The refinement of the Ge site occupancy factors converged to 95.9(2)% for Ge1 and 4.1(2)% for Ge1′. The lighter phenyl group carbon atoms corresponding to Ge1′ were not observed. The final refinement[43] included anisotropic temperature factors on all non-hydrogen atoms and converged to $R_1 = 0.0621$ and $wR_2 = 0.1381$. Structure solution and graphics were performed using SHELXTL PC. SHELX-93 was used for structure refinement and creation of publication tables.[44] Additional parameters are given in Table 6.

Table 6. Crystal Data and Structure Refinement for $Mo(CO)(\eta^2\text{-}SiH_2Ph_2)(depe)_2$, $MoH(GeH_2Ph)(CO)(depe)_2$, and $Mo(CO)(\eta^2\text{-}GeH_2Ph_2)(depe)_2$

	$MoH(GeH_2Ph)$	$Mo(\eta^2\text{-}SiH_2Ph_2)$	$Mo(\eta^2\text{-}GeH_2Ph_2)$
chem formula	$C_{27}H_{56}OP_4MoGe$	$C_{33}H_{60}OP_4MoSi$	$C_{33}H_{60}OP_4MoGe$
cryst color	yellow	red	colorless
fw	689.13	720.72	765.22
space group	*C*2/*c*	*Pbca*	$P2_1/c$
λ, Å	0.71073	0.71073	0.71073
temp (°C)	−70	−70	−73
a (Å)	33.061(4)	20.025(4)	10.1623(6)
b (Å)	10.6503(12)	17.348(3)	17.5501(9)
c (Å)	19.739(2)	21.743(4)	21.1247(11)
β (deg)	106.058(2)		98.712(1)
volume (Å^3)	6678.9(14)	7553(2)	3724.1(3)
Z	8	8	4
ρ_{calc} (g cm^{-1})	1.371	1.268	1.365
GOF	1.238	1.152	1.248
μ (cm^{-1})	1.485	5.72	0.1339
final *R* indices ($I > 2\sigma$)	$R_1 = 0.0403$	$R_1 = 0.0753$	$R_1 = 0.0621$
	$wR_2 = 0.0648$	$wR_2 = 0.1060$	$wR_2 = 0.1381$

A colorless, rectangular plate-shaped crystal of $MoH(GeH_2Ph)(CO)(depe)_2$, **4**, was mounted from a pool of mineral oil bathed in an argon gas flow and then immediately transferred to a liquid nitrogen vapor stream on the goniometer. A hemisphere of data was collected on a Bruker P4/CCD/PC using a combination of φ and ω scans, with 30 s frame exposures and 0.3° frame widths. The lattice parameters were determined from a least-squares refinement on 8192 reflections. Data collection, initial indexing, and cell refinement were handled using SMART[40] software. Frame integration and final cell parameter calculations were carried out using SAINT[41] software. Absorption corrections were performed using SADABS.[45] Data collection parameters are given in Table 6. The structure was solved in the space group *C*2/*c* using a combination of direct methods and difference Fourier techniques. The hydride and germanium hydrogen atom positions were found on a difference map, and the positions refined with isotropic temperature factors fixed at 0.08 Å^2. All other hydrogen atom positions were fixed in ideal positions; C−H = 0.96 Å (methyl), 0.97 Å (methylene), and 0.93 Å (aromatic). Fixed hydrogen

(34) Frisch, M. J.; Trucks, G. W.; Schlegel, H. B.; Scuseria, G. E.; Robb, M. A.; Cheeseman, J. R.; Zakrzewski, V. G.; Montgomery, J. A.; Stratmann, R. E.; Burant, J. C.; Dapprich, S.; Millam, J. M.; Daniels, A. D.; Kudin, K. N.; Strain, M. C.; Farkas, O.; Tomasi, J.; Barone, V.; Cossi, M.; Cammi, R.; Mennucci, B.; Pomelli, C.; Adamo, C.; Clifford, S.; Ochterski, J.; Petersson, G. A.; Ayala, P. Y.; Cui, Q.; Morokuma, K.; Malick, D. K.; Rabuck, A. D.; Raghavachari, K.; Foresman, J. B.; Cioslowski, J.; Ortiz, J. V.; Stefanov, B. B.; Liu, G.; Liashenko, A.; Piskorz, P.; Kamaromi, I.; Gomperts, R.; Martin, R. L.; Fox, D. J.; Keith, T.; Al-Laham, M. A.; Peng, C. Y.; Nanayakkara, A.; Gonzalez, C.; Challacombe, M.; Gill, P. M. W.; Johnson, B. G.; Chen, W.; Wong, M. W.; Andres, J. L.; Head-Gordon, M.; Replogle, E. S.; Pople, J. A. *Gaussian 98*; Gaussian Inc.: Pittsburgh, PA, 1998.

(35) (a) Lee, C.; Yang, W.; Parr, R. G. *Phys. Rev. B* **1988**, *37*, 785. (b) Becke, A. D. *J. Chem. Phys.* **1993**, *98*, 5648. (c) Stephens, P. J.; Devlin, F. J.; Chabalowski, C. F.; Frisch, M. J. *J. Phys. Chem.* **1994**, *98*, 11623.

(36) (a) Bartlett, R. J. *J. Phys. Chem.* **1989**, *93*, 1697. (b) Bartlett, R. J.; Watts, J. D.; Kucharski, S. A.; Noga, J. *Chem. Phys. Lett.* **1990**, *165*, 513.

(37) Hay, P. J.; Wadt, W. R. *J. Chem. Phys.* **1985**, *82*, 299.

(38) Höllwarth, A.; Böhme, M.; Dapprich, S.; Ehlers, A. W.; Gobbi, A.; Jonas, V.; Köhler, K. F.; Stegmann, R.; Veldkamp, A.; Frenking, G. *Chem. Phys. Lett.* **1993**, *208*, 237.

(39) (a) Hehre, W. J.; Ditchfield, R.; Pople, J. A. *J. Chem. Phys.* **1972**, *56*, 2257. (b) Hariharan, P. C.; Pople, J. A. *Theor. Chim. Acta* **1973**, *28*, 213. (c) Francl, M. M.; Pietro, W. J.; Hehre, W. J.; Binkley, J. S.; Gordon, M. S.; DeFrees, D. J.; Pople, J. A. *J. Chem. Phys.* **1982**, *77*, 3654.

(40) *SMART* Version 4.210; Bruker Analytical X-ray Systems, Inc.: 6300 Enterprise Lane, Madison, WI 53719, 1996.

(41) *SAINT* Version 4.05; Bruker Analytical X-ray Systems, Inc.: Madison, WI 53719, 1996.

(42) *SHELXTL PC* Version 4.2/360; Bruker Analytical X-ray Instruments, Inc.: Madison, WI 53719, 1994.

(43) R1 = $\Sigma||F_o| - |F_c||/\Sigma|F_o|$ and wR2 = $[\Sigma[w(F_o^2 - F_c^2)^2]/\Sigma[w(F_o^2)^2]]^{1/2}$. The parameter $w = 1/[\sigma^2(F_o^2) + (0.0669P)^2]$.

(44) Sheldrick, G. *SHELX-93*; University of Göttingen: Germany, 1993.

(45) Sheldrick, G. *SADABS*; University of Göttingen, Germany, 1996.

atom positions were refined using a riding model, with their isotropic temperature factors set to 1.5 (methyl) or 1.2 (aromatic, methylene) times the equivalent isotropic U of the carbon atom they were bound to. The final refinement[46] included anisotropic temperature factors on all non-hydrogen atoms and converged to $R_1(I > 2\sigma) = 0.0403$ and $wR_2(I > 2\sigma) = 0.0648$. Structure solution, refinement, graphics, and creation of publication tables were performed using SHELXTL 5.10/DOS software.[47] Additional details of the structure refinement are included in Table 6.

Red crystals of $Mo(CO)(depe)_2(SiH_2Ph_2)$ were obtained and analyzed on a Siemens P4S diffractometer. The data were collected at low temperatures using ω measurement methods, and an absorption correction was applied using psi-scan data. While the H's attached to the Si were easily located in the difference Fourier and refined well, there were residual peaks close to the Mo of equal height as a result of the data not being as good as for the other structures. Refinement was carried out on F^2 for all reflections except for five with very negative F^2 or those flagged by the user for potential systematic errors.

Acknowledgment. G.J.K. is grateful to the Department of Energy, Office of Basic Energy Sciences, Chemical Sciences Division, for funding. J.L.V. and S.L. thank the Director of the Los Alamos National Laboratory for postdoctoral funding. A.L., F.M., and J.T. acknowledge financial support from the Spanish "Dirección General de Investigación" (Project BQU2002-04110-CO2-02). The use of computational facilities of the Centre de Supercomputació i Comunicacions de Catalunya (C4) is gratefully appreciated also. We are also indebted to Ged Parkin for alerting us to a crucial crystallographic disorder phenomenon.

Supporting Information Available: X-ray crystallographic data for the structures of $Mo(CO)(GeH_2Ph_2)(depe)_2$, $Mo(CO)(SiH_2Ph_2)(depe)_2$, and $MoH(GeH_2Ph)(CO)(depe)_2$. This material is available free of charge via the Internet at http://pubs.acs.org.

OM030569J

(46) $R1 = \Sigma||F_o| - |F_c||/\Sigma|F_o|$ and $wR2 = [\Sigma[w(F_o^2 - F_c^2)^2]/\Sigma[w(F_o^2)^2]]^{1/2}$. The parameter $w = 1/[\sigma^2(F_o^2) + (0.0137P)^2]$.

(47) *SHELXTL* Version 5.10/DOS; Bruker Analytical X-ray Systems, Inc.: Madison, WI 53719, 1997.